Detailed Modeling and Simulation of Automotive Exhaust NO_x Reduction over Rhodium under Transient Lean-Rich Conditions

D I S S E R T A T I O N

submitted to the

Combined Faculties for the Natural Sciences and for Mathematics

of the Ruperto-Carola University of Heidelberg, Germany

for the degree of

Doctor of Natural Sciences

presented by

Qingyun Su, M.Sc.

Born in Linyi, Shandong, China

Examiners: Prof. Dr. Uwe Riedel

Prof. Dr. Jürgen Wolfrum

Heidelberg, June 26, 2009

Inderdisziplinäres Zentrum für Wissenschaftliches Rechnen

Ruprecht - Karls - Universität Heidelberg

2009

D I S S E R T A T I O N

submitted to the

Combined Faculties for the Natural Sciences and for Mathematics

of the Ruperto-Carola University of Heidelberg, Germany

for the degree of

Doctor of Natural Sciences

presented by

Qingyun Su, M.Sc.

Born in Linyi, Shandong, China

Heidelberg, June 26, 2009

T i t l e

Detailed Modeling and Simulation of Automotive Exhaust NO_x Reduction over Rhodium under Transient Lean-Rich Conditions

Examiners: Prof. Dr. Uwe Riedel

Prof. Dr. Jürgen Wolfrum

Detailed Modeling and Simulation of Automotive Exhaust NO_x Reduction over Rhodium under Transient Lean-Rich Conditions

Abstract: In this thesis, processes on a rhodium based catalytic NO_x decomposition/reduction system operated under periodic lean/rich conditions are considered. The kinetic behavior of this system is simulated using a module of the CFD package DETCHEM, which treats the transient processes in the chemically reactive flow and couples those to microkinetic simulations based on multi-step reaction mechanisms. A detailed reaction mechanism over rhodium is extended and presented. The mechanism consists of oxidation reactions of CO and hydrogen and reduction reactions of NO_x. The impact of temperature and temporal periods of the lean and rich phases on conversion of the pollutants is discussed. The trends of the experimentally observed and numerically predicted dynamic behaviors of the catalytic system agree well. The model could be applied in the design/optimization of catalytic exhaust after-treatment devices. Furthermore, this work potentially contributes to the development of applicable catalysts for vehicles equipped with diesel engines, lean-operated gasoline engines such as gasoline direct injection (GDI) engines.

Detaillierte Modellierung und Simulation von rhodiumbasierten Abgaskatalysatoren zur NO_x-Reduktion unter periodisch wechselnden mageren/fetten Bedingungen

Zusammenfassung: In dieser Arbeit wird ein auf Rhodium basierendes Katalyseverfahren für den Zerfall bzw. die Reduktion von NO_x untersucht. Hierbei werden die periodisch wechselnden mageren/fetten Bedingungen berücksichtigt. Die Kinetik dieses Systems wird mit der CFD-Software DETCHEM simuliert. Dabei werden die Übergangsprozesse in der reaktiven Strömung mit mikrokinetischen Simulationen, die auf Vielschritt-Reaktionen beruhen, gekoppelt. Ein detaillierter Reaktionsmechanismus für die Rhodiumkatalyse wird erweitert und präsentiert. Dieser beinhaltet Reaktionen für die Oxidation von CO und Wasserstoff und die Reduktion von NO_x. Der Einfluss der Temperatur und der periodischen mageren/fetten Phasen auf die Umwandlung der Schadstoffe wird diskutiert. Ein Vergleich, der mit diesem Mechanismus erstellten Simulationen mit den experimentell erhaltenen Messdaten zeigt eine gute qualitative Übereinstimmung. Dieses Modell kann somit zur Entwicklung und Optimierung katalytischer Abgasreinigungssysteme genutzt werden. Darüber hinaus kann diese Arbeit dazu beitragen die Entwicklung von Katalysatoren für Fahrzeuge mit Diesel, und Benzin-Direkteinspritzermotoren (GDI) voranzubringen.

Contents

Chapter 1: Introduction

In this chapter, the background and objectives of the research presented in this dissertation are given.

"If we knew what it was we were doing,
it would not be called research, would it?"

--Albert Einstein

Environmental, ecological, and health concerns call for increasingly stringent emissions regulations of pollutants [1]. These regulations include limits on nitric oxides (NO_x), carbon monoxide (CO), hydrocarbon (HC) and particulate matter (PM) emissions from the exhaust gas of vehicles. Although the emissions of global warming potential greenhouse gases (GWP-GHG), such as CO_2 and nitrous oxide (N_2O), are not regulated at present, they are also under increasing scrutiny. For example, since 1995 there has been an agreement by the ACEA[1] promising to reduce CO_2 emissions of newly marketed automobiles by 25% by the year 2008 compared to 1995 [2]. Meanwhile, the shortage of fuel and the energy crisis lead us to develop fuel-efficient vehicles. One way to reduce CO_2 emissions and coincidentally improve

[1] European Automobile Manufacturers' Association

overall fuel economy, is the use of lean-burn engines [1]. Lean-burn gasoline, natural gas and diesel engines cannot meet the future more and more stringent regulations on NO_x and PM emissions by improving the internal combustion only. Upcoming Environmental Protection Agency (EPA) and European Union (EU) legislations require further significant reductions in NO_x and particulate matter emissions especially from diesel engines.

The design of catalytic converters for specific applications requires an accurate knowledge of reaction kinetics including CO oxidation, NO reduction, etc. under not only steady-state, but also more importantly, instationary conditions. Most currently available kinetic models are valid only under steady-state conditions but cannot properly describe the effects of rapid changes in exhaust composition and temperature.

In a preliminary study, it was found that the existing quasi-elementary step reaction mechanism on rhodium could not adequately and accurately describe the transient behavior of the catalytic NO_x decomposition system proposed by Nakatsuji [3]. Furthermore, it is believed that the strong dependence of reaction mechanism and kinetics on adsorbate coverage is an important factor behind the large differences in activation energies and pre-exponential factors as reported in the literature [4, 5].

Hence, the motivation of this thesis is to develop an improved detailed mechanistic model, which will be validated using the transient simulations to account for the coverage-dependent reaction parameters, and to bridge the gaps between the model catalyst under the steady-state conditions and the real-world automotive exhaust gas catalyst under the instationary conditions.

The main objective of this research is the development of a detailed microkinetic model to simulate and elucidate the transient processes during the two-phase lean/rich periodic catalytic decomposition of NO_x with CO, H_2, hydrocarbons, *e.g.* C_3H_6 as reductants. The mechanism developed in this work is utilized to simulate the whole system with the DETCHEM^{TRANSIENT} code [6]. The phenomenological UBI-QEP method[2] [7, 8], which is in a thermodynamically consistent way was taken to calculate the heats of chemisorption, the reaction enthalpies and the reaction activation energies for several elementary reaction networks for CO-O_2, H_2-O_2, NO-O_2, and C_3H_6-O_2 systems over rhodium.

[2] Unity Bond Index-Quadratic Exponential Potential method, developed from formerly known BOC (Bond Order Conservation) method by Evgeny Shustorovich et al. [7].

This thesis focuses on detailed transient modeling study of the automotive exhaust after-treatment catalytic converter. The transient behavior of the NO decomposition over a rhodium based catalyst is investigated in detail. The model system studied is periodic and consists of two steps: an operation in oxidizing conditions and a relative short operation in reducing conditions with a CO (or H_2) pulse-injection.

A series of model exhaust gases, viz. $CO\text{-}O_2$, $NO\text{-}O_2$, $CO\text{-}NO\text{-}O_2$, $H_2\text{-}NO\text{-}O_2$, $C_3H_6\text{-}NO\text{-}O_2$ over rhodium are studied in this thesis.

The detailed kinetic model developed in this thesis consists of five separate sub-models:

(1) oxidation of CO,
(2) oxidation of H_2,
(3) reduction of NO,
(4) oxidation of NO,
(5) oxidation of propene (C_3H_6).

The model could be applied in the design/optimization of catalytic exhaust after-treatment devices. Furthermore, this work potentially contributes to the development of applicable catalysts for vehicles equipped with diesel engines, lean-operated gasoline engines, such as gasoline direct injection (GDI) engines, and lean-burn natural gas engines.

The thesis is organized as follows:

The fundamentals on the exhaust gas after-treatment and the current $DeNO_x$ technology are introduced in Chapter 2. In the following, Chapter 3 introduces the concept and fundamentals for modeling heterogeneous reactive flows and the computational tools used for the current numerical simulation are described. Also included are the methods and the process of constructing a detailed elementary surface reaction mechanism. Later in Chapter 4, the simulation results, as well as the comparison with experimental results are presented for the transient processes during the catalytic reduction of NO_x with CO, H_2, and hydrocarbons (e.g. C_3H_6) as reductants. Finally, conclusions and outlook are given in Chapter 5.

Chapter 2: Automotive Exhaust Gas After-treatment

In this chapter, the fundamentals on the exhaust gas pollutants after-treatment are given. The background knowledge of NO_x formation and the particulate matter versus NO_x trade-off are given. The state-of-the-art technology for the catalytic reduction of NO_x from the automotive exhaust gas is presented and discussed. The cold-start problem and the transient studies as one solution to it are also discussed.

2.1 Introduction

It is found out that combustion engines are a major source of harmful pollutants. For example, gasoline is a mixture of hydrocarbons containing roughly 20% butanes and pentanes, 35% aromatic compounds, and 45% alkenes and alkynes [9]. Under ideal conditions, the combustion of gasoline in air should produce only water (H_2O) and carbon dioxide (CO_2), together with the nitrogen (N_2) from the air. However, no combustion is ideal. In addition to these main products of combustion, the engine exhaust also contains thousands of different compounds, in particular, gaseous nitric oxides (NO_x), carbon monoxide (CO) and hydrocarbons (HCs) emissions and the solid particulate matter (PM). Nitrous oxide (N_2O) has

gained increasing attention as a dangerous environmental pollutant due to the destruction of stratospheric ozone and also as a greenhouse gas [10].

2.1.1 NO_x emissions from combustion

NO_x is the generic name for nitrogen monoxide, also referred as nitric oxide (NO) and nitrogen dioxide (NO_2). NO_x normally does not include N_2O. NO and NO_2 are in equilibrium with each other in the presence of O_2, while the former is favored at higher temperatures, such as in combustion chambers and their immediate surroundings, whereas the latter is favored under normal atmospheric conditions. Thus in the diesel exhaust gas, the NO_2 content is only about 5-10% of total NO_x [11], while in the case of gasoline, about 8%. As a rule, most experimental studies make use of model reaction mixtures based on NO. However, what is met in actuality is a mixture of oxides (NO, NO_2) [12].

NO_x originates mainly from the combustion processes and is formed via four basic reaction routes [13]. Each of the formation routes may have relative proportions contributed to the total NO_x concentration, and are dependent on combustion temperature, residence time, air to fuel ratio (AFR) and fuel type.

During combustion the temperature of flame front is so high (1600 °C or even higher) that the endothermic equilibrium between nitrogen (N_2) and oxygen (O_2) to form nitric oxide (NO) is established. Subsequent rapid cooling and ejection of the combusted gas into the exhaust system freezes this equilibrium, so exhaust gas still contains significant levels of NO [14].

NO_x can cause the formation of photochemical smog and acid rain, and hence is a threat to people's health and environment. Since a large portion of NO_x is originated from combustion in mobile vehicles, such as cars and trucks, the minimization of NO_x from the engines is thus of great significance. As described above, the reduction of NO_x under lean (oxygen rich) conditions remains challenging.

2.1.2 NO_x-particulate trade-off

The control of particulate matter (PM) emissions together with NO_x represents significant challenges to the Diesel engine manufacturers. This is the well-known trade-off between PM and NO_x. Generally, when the engine operates at low load and hence lower temperatures, it

produces less NO_x but more PM. However, at higher temperatures combustion is more complete, cause less PM but more NO_x formation due to the extended Zeldovich mechanism (thermal NO production). In recent years, exhaust gas recirculation (EGR) has been studied for use in Diesel engines to reduce the emissions of NO_x. The exhaust gas dilutes the combustion process and lowers the temperature, and hence lowers the NO_x production. However, EGR causes soot to increase.

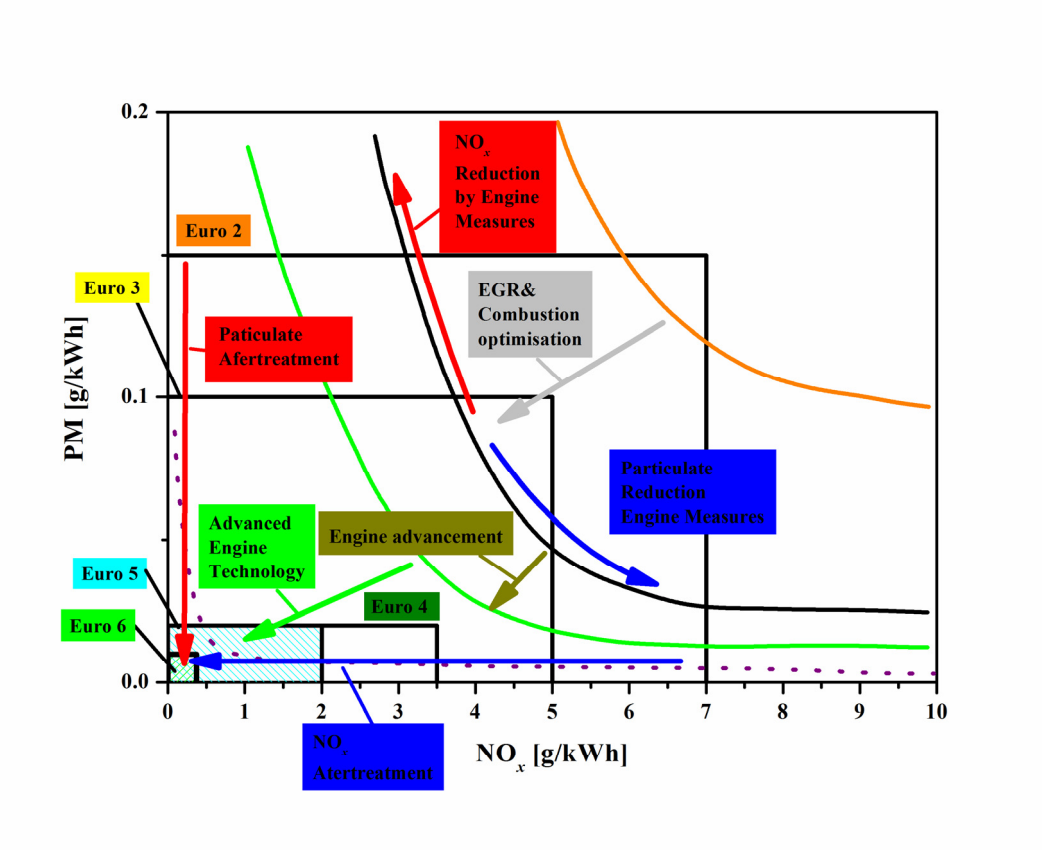

Figure 2-1 Illustration to NO_x-particulate matter trade-off curves in the Diesel engine.

It is common to plot particulate matter against nitrogen oxides, because this focuses on the trade-off between these two pollutants, see Figure 2-1. This trade-off is once the bottleneck for further decreasing the pollutants of particulate (soot) and NO_x simultaneously from the diesel engine. However, it is not a constant relationship. In fact, over a period of time, developments in engine technology have allowed and continue to allow the trade-off curve to move to lower values of both NO_x and PM. The upper outer curve (in orange color) can be shifted to the inner curve (in dark black), and so on, as shown in the graph. It suggests that as European Union (EU) pollutant emission regulations evolves from Euro 2 to Euro 6, different approaches can be taken to lower the tailpipe emissions to below targeted limits.

2.1.3 Historic overview of pollution control regulations

The first emission legislation was enacted in 1959 in California, followed by the first US Federal standards in 1966, and Japan in 1966. Subsequently, the first regulation "Regulation 15" was introduced in Europe in 1970. Over the past years, countries around the world have gradually imposed increasingly stringent emission regulations on the motor industry. Nowadays all of the industrialized countries and many developing countries have some forms of regulations for the vehicle emissions [15]. For example, the European limits for diesel engine powered passenger cars are becoming more and more tightening, as shown in Figure 2-2 [16].

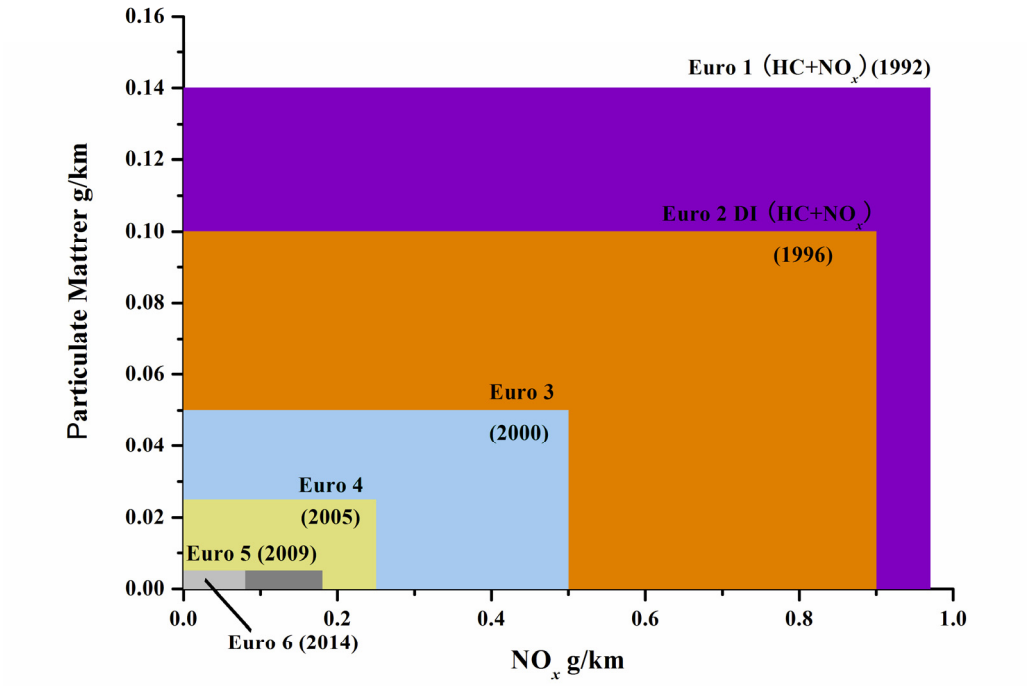

Figure 2-2 Gradual tightening of European emission standards for DI diesel engine passenger cars (for Euro 1 and Euro 2 emission levels, 'NO_x' values correspond to the sum of NO_x and HC emissions) (After [16]).

In China, the introduction of the regulation is comparatively late (around 1979), while the progress is rather rapid. China currently adopts the "National step 3" emission standards (equivalent to Euro III). Next "National step 4" (Euro IV) emission standards are planned to be implemented (those currently prevailing in the EU) throughout China from 2010, though it has been in trial implement on the public transportation and utility vehicles in Beijing before

the Olympic Games in 2008. It is anticipated that the Chinese future regulations will be nearly at the same level as that of Europe's around 2014, while the Euro VI regulation will come into effect.

The limits which regulatory bodies impose are often described as "technological force", which means that the industry is compelled to undertake the research and development (R&D) to create emission control technology [17].

In the early days, the industry could manage to meet tailpipe limits by the primary method of adjusting and improving the combustion system. However, with the constant tightening of the emission regulations, it eventually became impossible to satisfy legislations if not combined with a secondary measure. Clearly some new approaches were needed, leading to the introduction of exhaust gas "after-treatment". This term means a clean-up of the exhaust gas between its expulsion from the engine and emission from the tailpipe [17]. Nowadays after-treatment is a very important measure to clean the exhaust gas as the final stage before the gas traversing exhaust pipe.

2.1.4 Success and significance of pollution control

It has now been over 30 years since the introduction of the catalytic converter to reduce emissions from internal combustion engine. It is considered as one of the greatest environmental successes of the 20^{th} century. However, new emission control technologies are still being developed to meet ever more stringent mobile source (both gasoline and diesel engines) emissions. Catalyst-based control technology, which has played a critical role in these successes, will continue to play a major role in meeting the future challenges.

The benefits of catalytic control units have been documented. It was estimated that by the year 2000, over 800 million tons of combined pollutants of HC, CO and NO_x had been abated using auto exhaust catalyst and prevented from entering the atmosphere [18]. Another example is that, thanks to the motor vehicle emissions control program, the ambient air in the U.S. is much cleaner than it was 30 years ago even though the U.S. resident population has increased by 33%, vehicle miles traveled have increased by 140% and the gross domestic product has increased by 147% meanwhile [19].

2.2 Catalytic Exhaust NO_x After-treatment

The reduction of NO_x in exhaust emissions from mobile and stationary sources is one of the key environmental problems of our century [20-22]. Depending on the relative oxygen content in the exhaust, there are several proposals for NO_x control. The stoichiometry number, S, is used to identify the redox characteristics of the model exhaust gas. When S<1, S=1 and S>1, the simulated gas is net reducing (fuel rich), stoichiometric, and net oxidizing (fuel lean), respectively.

The catalytic converters were first introduced in the USA in 1975, and were designed to control (oxidize) the two pollutants only: unburned hydrocarbons and carbon monoxide. Therefore, from its functions of oxidation, the early (first) generation of the converter was named as "oxidation catalyst". Three-way catalyst (TWC) was first installed in 1979 [9]. Today, the latest generation of TWC functions quite well under stoichiometric conditions.

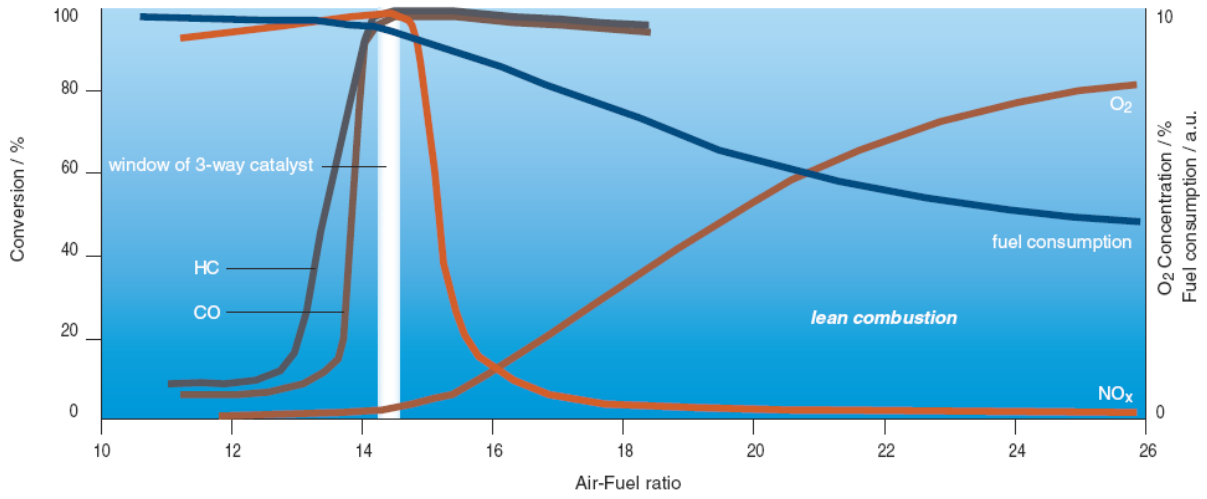

Figure 2-3 Fuel consumption and 3-way performance of a gasoline engine as a function of air–fuel (A/F) ratio [23].

The lean operation of the diesel engine and lean-burn gasoline engine give rise to high fuel efficiency that, in turn, decreases CO_2 emissions that contributes to the "greenhouse" effect [24]. However, the TWC does not apply to the lean-burn engine exhaust conditions because of the vast excess of oxygen, see Figure 2-3 [23]. There are variable systems under development for the NO_x control for such lean-burn systems. According to the running conditions, they are divided into full lean systems and mixed lean/ rich systems. Extensive

researches have focused on the study of converting the nitric oxides into harmless nitrogen. Among them, the catalytic reduction/decomposition of NO_x is a very promising solution of the problem. However, the quick deactivation of this system is inevitable due to the accumulation of the adsorbed oxygen left after NO decomposition. The goal is to find a catalyst that efficiently converts NO_x selectively to N_2 under lean-burn conditions, is not deactivated by sulfur, and furthermore does not decrease the fuel efficiency.

2.2.1 NH_3-SCR for lean NO_x reduction

Selective catalytic reduction of NO_x with ammonia or urea (NH_3-SCR) is currently employed as an effective NO_x removal technology for stationary power stations working under a vast excess of oxygen. NH_3-SCR is based on the reaction of NO_x from the engine with injected of NH_3 to selectively produce N_2 and water, as Equation 2.1. This reaction is catalyzed by a mixture of metal oxides, e.g. V_2O_5, TiO_2 and WO_3.

$$6NO+4NH_3 \rightarrow 5N_2+6H_2O \qquad 2.1$$

Although NH_3-SCR is highly efficient, it requires on-board facilities to store urea and is hence not well feasible for the application in automobiles [12].

2.2.2 HC-SCR for lean NO_x reduction

Selective Catalytic Reduction with hydrocarbons (HC) as reductant (HC-SCR) has been studied extensively [22]. A passive HC-SCR system utilize hydrocarbons (HC) emitted by the combustion engine, while the active HC-SCR uses the additional external HC as reductant by injection, e.g. diesel fuel in the case of Diesel engine. Yet the main shortcomings of HC-SCR are low activities, severe deactivation by H_2O (i.e., low hydrothermal stability), and poor selectivity towards nitrogen. What is more, HC-SCR catalysts, in particular with platinum, convert much NO_x to N_2O, which is a high global warming potential green house gas.

2.2.3 NO_x Storage and Reduction (NSR) Catalyst

An entirely different and relative new approach is the NO_x Storage-Reduction (NSR) catalyst, which is also known as lean NO_x trap (LNT) or NO_x storage catalyst (NSC). It stores NO_x during lean phases and releases and subsequently reduces it during rich phases. Herewith NO_x emission can be abated efficiently, for long period in presence of low SO_x concentrations.

However, continuous exposure to SO_x will deteriorate the NSR due to the irreversible adsorption of SO_x on the NO_x adsorption sites [25]. Normally the NSR system needs periodic regeneration for the catalyst with additive fuel to recover its activity, thus decreasing the fuel economy.

2.2.4 Nakatsuji-type cyclic NO_x decomposition catalyst

Several years ago, Nakatsuji *et al*. [3, 26] proposed a rhodium-based catalytic NO_x reduction system which, when operated under periodic lean-rich conditions, can reduce NO_x efficiently and endure the exposure to sulfur components. Therefore, this system has a high potential for application in automobiles. However, it deteriorates for reasons not completely understood yet. Furthermore, the detailed surface mechanism of this system is unclear.

This system is one of the topics of the project "Catalytic removal of NO_x and soot particles from the exhaust gas of diesel engines" within Competence Network Catalysis (ConNeCat) initiated by the German Federal Ministry for Education and Research (BMBF). It will be discussed in detail in this thesis, in parallel to the doctoral thesis that finished earlier by Inderwildi [27].

2.3 Challenges: unresolved important problems

2.3.1 The cold-start problem

Combustion emissions from the engine exhaust during the warming-up period has received much attention in recent years. Many researches have shown that the emissions during that period consist most of the cycle, which is called the cold-start problem. More than 80% of the emissions from cars equipped with catalysts come from the first three minutes of driving during a cycle [28]. During the "cold-start", the exhaust released from the engine of a car will pass the catalyst without purification. The reason for this is that the catalyst is inactive at low temperatures [29]. It is suggested that this inactivity of the catalyst at low temperatures arises from self-poisoning of different compounds, e.g. CO or hydrocarbons adsorbed on the catalyst surface [30].

Furthermore, at low temperatures much NO_x is converted to N_2O rather than N_2 with the catalytic converter by platinum group metals. That is to say, the N_2O selectivity is very high at low temperatures.

For low-temperature exhaust emissions there is much interest in developing new catalytic technology [31]. It is desired to develop an efficient catalyst that has lower light-off temperature, at which the conversion of 50% is achieved. One alternate way is therefore to find techniques that can minimize the self-poisoning and thus can convert the emissions at low temperatures immediately after a cold start of the engine [29].

2.3.2 The transient gas composition modulation

One way to partly solve the above-mentioned cold-start difficulty and improve the light-off performance is changing the gas compositions [32]. By changing the gas compositions, the light-off performance at low temperatures is improved [32]. For example, in a recent experimental study [29], a substantial improvement of the low temperature oxidation activity was observed for both a commercial and a model catalysts by introducing well-controlled periodic O_2 pulses to simple gas mixtures of CO or C_3H_6 (diluted in N_2).

However, the underling mechanism is still poorly understood for the three-way catalyst (TWC) and especially the lean $DeNO_x$ catalyst working under transient conditions, which will be one of the objectives of the thesis in the following chapters.

2.3.3 Transient modeling and simulation study

In recent years transient experiments are becoming a powerful tool for gaining insight into the mechanisms of complex heterogeneously catalyzed reactions and to derive rate constants for the individual steps involved [33]. This is mainly because the steady-state behavior can often be described by several distinct models, contrary to the dynamic behavior, which is much more model-sensitive. That is, kinetics measured under steady-state conditions lead to overall models unable to predict the dynamic behavior of those systems. To study instationary behavior of the kinetic system, various techniques were utilized. The pulse injection techniques were always used since it would yield kinetic information which is not obtainable from steady-state experiments [34]. Therefore, the instationary operation is useful for the discrimination between different reaction models [35, 36].

Such experiments conducted in the transient regime permit the quantitative determination of the surface composition during catalysis and also give important information on the sequence of steps that underlie the observed global reaction [37].

Results from transient experiments lead to reliable models for reactor design, and they are essential for reactors operating in the transient regime, a situation becoming increasingly common [37]. Therefore, it is possible to conduct computer-based modeling and simulation, combining the wealth of the transient experimental results to validate the kinetic models. Thus, the behavior of the reacting system can be simulated by numerical methods over a wide range of variables.

Although there are a variety of experimental studies on the transient behavior as cited above, the mechanistic studies are scarce [36]. Therefore, the modeling and simulation coupled with a detailed mechanism are highly needed for the transient heterogeneous catalytic system, which is one of the objectives of this work.

Chapter 3: Modeling and Simulation of a Catalytic Monolith

In this chapter, the fundamentals on the physical and chemical bases for the research described in this thesis are given. The computational fluid dynamics (CFD), the catalysis, the computer code used in this work and the boundary layer approach are outlined. The method to construct the detailed mechanism is presented. The microkinetic model is set up based on the available kinetic data from the literature and calculated in this work..

3.1 Modeling of surface reaction kinetics

The greatest challenge for the catalytic reaction modeler is the knowledge of the reaction kinetics [38]. In this thesis, we will focus on the heterogeneous surface reactions, since the homogenous gas-phase reactions usually can be neglected in automotive catalytic converters due to the relatively low temperature, low pressure and short residence time. For the implementation of gas-phase chemistry the interested reader is referred to [39].

Herein, surface and gas-phase reaction source terms are modeled by elementary-step-like reaction mechanisms using the corresponding module of the DETCHEM program package [40]. Heterogeneous reaction mechanisms include adsorption, desorption of atoms and

molecules, dissociation and formation of reactants and products. In the model approach, it is assumed that the adsorbed species are randomly distributed on the surface and that one can average over local inhomogenities, which is according to the so-called mean-field-approximation (MFA) approach. Then a rate law of the heterogeneous reactions can be written similar to the usual gas phase kinetics according to the mass action law.

The production rates $\dot{s}_i$ of surface and gas phase species (due to adsorption and desorption) are then written as

$$\dot{s}_i = \sum_{k=1}^{K_s} \nu_{ik} k_{f_k} \prod_{i=1}^{N_g+N_s} (c_i)^{\nu'_{ik}} \quad . \tag{3.1}$$

Here is K_s = total number of surface reactions including adsorption and desorption, ν_{ik}, ν'_{ik} = stoichiometric coefficients, k_{f_k} = forward rate coefficient, $N_g\,(N_s)$ = number of gaseous (surface) species, c_i = concentration of species *i*, which is given in, e.g., mol·cm^{-3} for gas phase and mol·cm^{-2} for adsorbed species.

The rate coefficient is expressed in a way that takes into account the coverage-dependence, since the binding states of adsorption on the surface vary with the surface coverage of all adsorbed species, which will be addressed in this work:

$$k_{f_k} = A_k\, T^{\beta_k} \exp\left[\frac{-E_{a_k}}{RT}\right] \prod_{i=1}^{N_s} \Theta_i^{\mu_{ik}} \exp\left[\frac{\varepsilon_{i_k}\Theta_i}{RT}\right] \quad , \tag{3.2}$$

where, A_k, preexponential factor, β_k, temperature exponent, E_{a_k}, activation energy of reaction *k*, and Θ_i, surface coverage of species *i*. The parameters μ_{i_k} and ε_{i_k} describe the dependence of the rate coefficients on the surface coverage of species *i*.

Chemical adsorptions are also chemical reactions since they include a rearrangement of bonding. Not only surface reactions but also adsorption processes depend on the surface coverage as well as on the chemical nature of the surface adsorbants. For adsorption reactions, sticking coefficients are commonly used. They are converted to conventional rate coefficients by:

$$k_{f_k}^{ads} = \frac{S_i^0}{\Gamma^\tau}\sqrt{\frac{RT}{2\pi M_i}} \quad , \qquad 3.3$$

with S_i^0: initial sticking coefficient, Γ : surface site density, e.g., in mol·cm^{-2}, τ: number of sites occupied by the adsorbing species, M_i : molar mass of species *i*. Usually, under most cases the adsorption is considered to be non-activated, as in Equation 3.3. However, some adsorption is considered to be activated and the activation energy and sticking coefficient are coverage-dependent, at least under some conditions, thus modification similar to Equation 3.2 is needed. An example for oxygen adsorption activated on rhodium catalyst under higher oxygen coverage is given later in this thesis as Inderwildi *et al*. suggested [5].

3.2 Simulation of the transient reactive flows - DETCHEM^{TRANSIENT} [3]

The simulation of the transient behavior of reacting fluids inside catalytic converters is a significant challenge. While considerable progress has been made with steady-state models, which contributed to the understanding and development of catalysts [41], it is necessary to develop models for the dynamic behavior of reacting fluids inside a converter in a relatively simple and efficient way [41-43]. The computer code DETCHEM^{TRANSIENT}, a module of DETCHEM [6], which simulates the transient processes inside a single channel of a catalytic converter rather computation time efficiently, was developed by Inderwildi *et al*. [27] for the simulation of the periodic lean-rich catalytic system.

3.2.1 Structure of DETCHEM

The DETCHEM applies elementary-step reaction mechanisms in the gas-phase and on catalytic surfaces in its CFD codes [6]. For instance, Tischer *et al.* [6, 44] developed DETCHEM^{CHANNEL}, a module that simulates annular flows such as the flow inside tubular reactor, *e.g.* channels in a honeycomb monolith, according to a boundary layer approach to the Navier-Stokes equations [45], see Figure 3-1 for the interaction between DETCHEM^{CHANNEL} and DETCHEM.

[3] This part on code development is mainly done by Inderwildi.

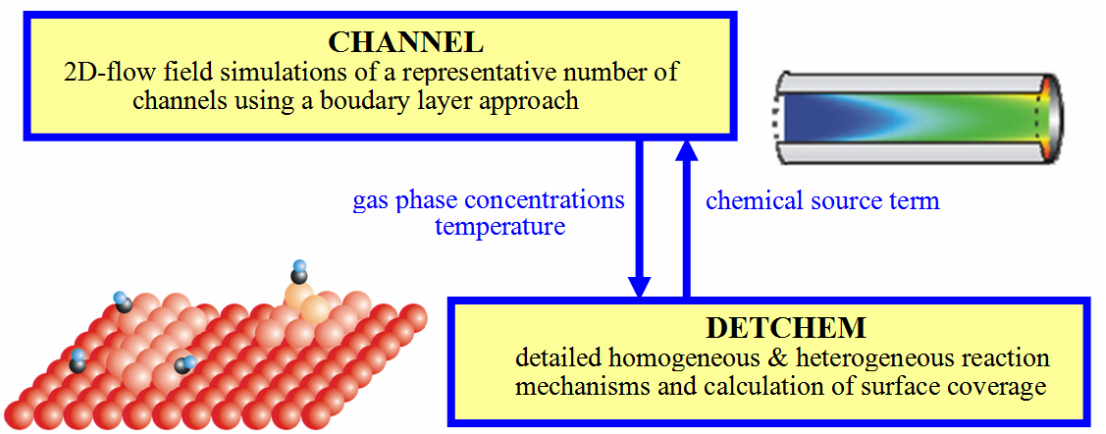

Figure 3-1 Structure of DETCHEM showing the interaction of the CHANNEL module and the main program DETCHEM.

3.2.2 Structure of DETCHEM^{TRANSIENT}

Even though transient processes in heterogeneous catalyst can be simulated by commercially available Navier-Stokes-based codes such as FLUENT [45], fully coupled models based on detailed surface chemistry are generally not applicable owing to the stiffness of the mathematical description and the consequently high CPU costs [46]. Based on the idea of time scale decoupling according to a hierarchical approach [27], the transient inlet gas composition (time scale of seconds) can be regarded as decoupled from the flow, since the residence time of the gas inside the reactor is much shorter (time scale of milliseconds). Furthermore, the flow field in the catalyst can be assumed as quasi-steady-state during the time step necessary for the accurate resolution of the surface chemistry.

The transient kinetic behavior of a catalytic converter was studied using this code, which couples time-dependent microkinetic simulations of surface reactions to a dynamic flow field. In the presented work, DETCHEM^{TRANSIENT} utilizes DETCHEM^{CHANNEL} to simulate the transient behavior of a catalyst operated under altering fuel lean/rich conditions. In case of automotive catalytic converters, gas-phase reactions usually can be neglected for reasons given at the beginning of this chapter. Therefore, only the implementation of surface chemistry in DETCHEM is discussed here.

3.2.3 Implementation of Transient Surface Chemistry

The surface processes investigated in this work are time-dependent and do not reach a steady-state. Therefore, not only the surface coverage, but also the temporal variation of the surface coverage is of interest here. The surface site density Γ is the number of adsorption sites per surface area A, e.g., in mol·cm^{-2}.

The time-dependent variation of the coverage, θ_i, of each adsorbed species i can be calculated from the molar production rates $\dot{s}_i$ (Equation 3.1) due to surface reactions, adsorption, and desorption according to

$$\frac{\partial \theta_i}{\partial t} = \frac{\dot{s}_i \sigma_i}{\Gamma} \quad . \qquad 3.4$$

Herewith, the surface coverages can be updated by integrating Equation 3.4. σ_i is the number of surface sites occupied by one particle of the adsorbed species i. A conservation relation for the solutions of Equation 3.4 is

$$\sum_{i=1}^{N_{ss}} \theta_i(t) = 1 \qquad 3.5$$

for any given t.

3.2.4 Coupling of the Transient Surface Chemistry to other Processes

The transient surface kinetics is coupled to the dynamic flow field using continuous feedback method in a hierarchical approach. A schematic overview on the interplay of the different DETCHEM modules for transient simulation is given in Figure 3-2. The different steps are explained in detail in the text; the step numbers are given in Figure 3-2 beside the head of the arrow corresponding to the calculation step.

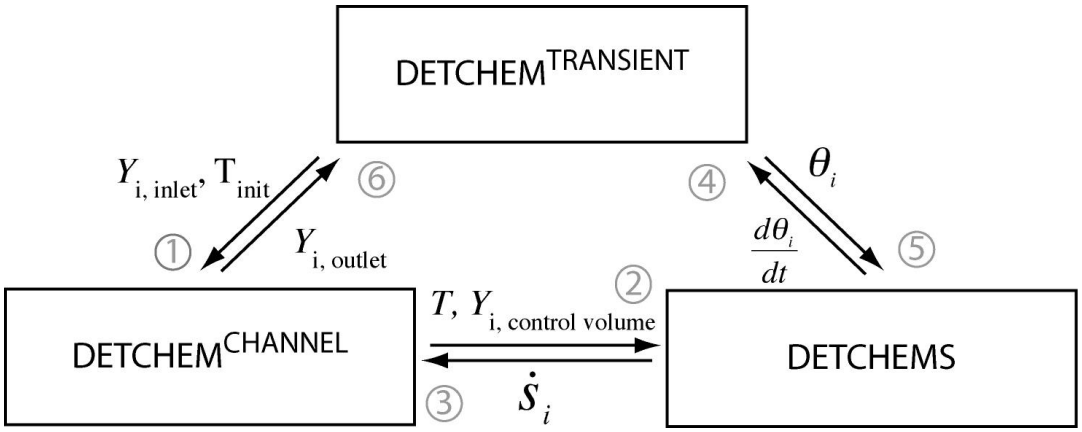

Figure 3-2 Schematic overview over the implementation of transient reacting flow simulation by DETCHEM [27]. The meaning of the various variables is given in the text.

DETCHEM^{TRANSIENT} initializes DETCHEM^{CHANNEL} with the initial temperature and inlet gas composition at t_0 provided by the user (step 1). Subsequently, DETCHEM^{CHANNEL} calculates the flow within the tubular reactor, based on the initial temperature and inlet gas composition. The gas-phase species concentrations calculated by DETCHEM^{CHANNEL} provide DETCHEMS with basis for the calculation of surface reaction rates (step 2). The production/consumption of species is then coupled to the flow field (step 3). DETCHEMS provides DETCHEM^{TRANSIENT} with the temporal variation of the surface coverages (Equation 3.4, step 4), which is integrated by DETCHEM^{TRANSIENT}. The absolute surface coverage is then utilized by DETCHEMS as initial value for the next time step (step 5) and furthermore documented to a text file. The calculated outlet gas composition is finally provided to DETCHEM^{TRANSIENT} by DETCHEM^{CHANNEL} (step 6). Both surface coverage and outlet gas composition at each time step is filed by DETCHEM^{TRANSIENT}. The inlet gas composition is then adjusted for the subsequent time step according to the input data provided by the user.

The described iteration is carried out for each time step. It will be shown later that this approach provides results in agreement with experimental investigations (See Chapter 4). In case of catalytic combustion, it was already shown by Raja *et al.* [46] that the accuracy of the boundary layer approach does not differ much from that of the full Navier-Stokes approach, while calculations based on the former approach consume considerable less computation time. Next to the input data for DETCHEMS and DETCHEM^{CHANNEL}, the user has to provide DETCHEM^{TRANSIENT} with the different species concentrations of the inlet gas ($Y_{i,\,\mathrm{inlet}(t)}$), the duration of both phases, the time step Δt and the initial surface coverage $\theta_i(t_0)$. As output,

DETCHEM^{TRANSIENT} creates files with the species concentrations in the outlet gas as a function of time $Y_{i,\ outlet(t)}$ and the surface coverage as a function of time and axial position $\theta_i(z, t)$.

3.3 Mechanism development approaches

3.3.1 Bridging the pressure gap as well as the material gap

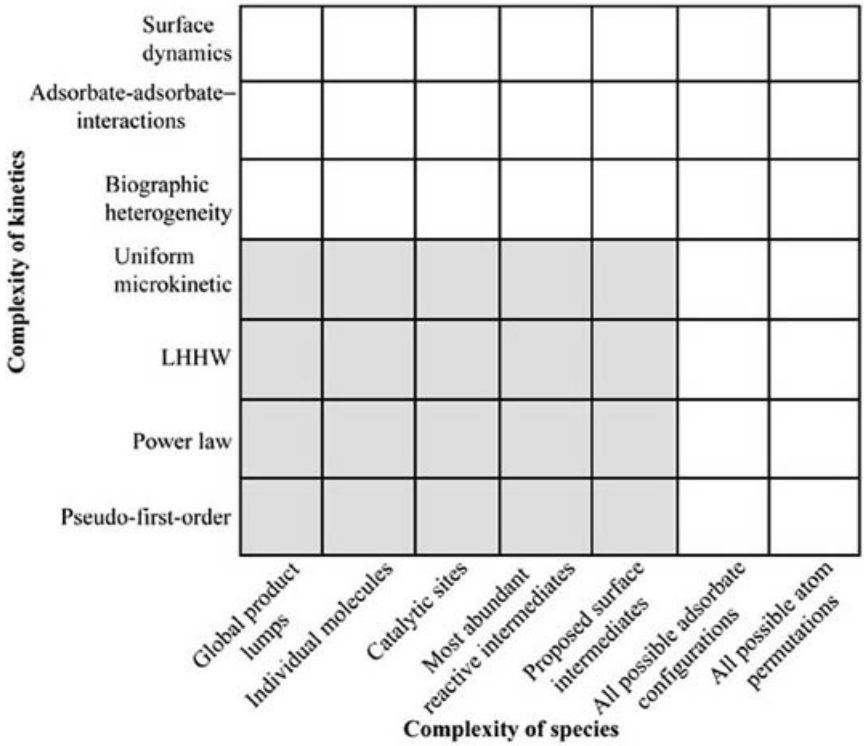

Figure 3-3 Matrix of complexity for kinetic modeling of heterogeneous catalytic chemistry [47]. The majority of the models developed to date are restricted to the lower left-hand corner of the matrix in the first five columns and the first four rows denoted by the shaded area.

Surface science experiments utilize numerous techniques to study adsorption, surface diffusion, reactions, desorption, and sometimes surface reconstruction. Most experimental studies are undertaken under either very low pressure (mostly at ultrahigh vacuum (UHV)) or off-line (unrealistic) conditions on well-defined model catalysts. Thus, there are two so-called

gaps exist, i.e. the pressure gap and the material gap between the studied system and the real system. For example, using optical sum-frequency generation (SFG) vibrational spectroscopy (see e.g., [48]) it was recently demonstrated that carbon monoxide can dissociate on platinum (see e.g., [49]) and on rhodium (see e.g., [50]) at high pressure and high temperature, while this reaction pathway could not be observed in numerous UHV experiments before. Therefore, the extrapolation of the results to real conditions, *i.e.* higher pressure as well as polycrystalline and supported catalysts, is much desired. During last few years, the surface science community has gained great advances in bridging the pressure and material gaps [48, 51]. This contributes considerably to the discovery of more accurate heterogeneous reaction mechanism.

It is nicely shown from Figure 3-3 [47] that the kinetics of heterogeneous catalyzed reactions is very complex, and nowadays we have only touched the simplest aspects and step by step to more realistic phenomena, not yet the real surface dynamics.

3.3.2 Microkinetic modeling

Since literature on the complex reaction mechanisms is usually very limited, various approaches are used to this end. Dumesic *et al.* [52] use the microkinetic method to study different reaction systems. The aim of the microkinetic approach to a gas/solid catalytic reaction is to determine and combine the kinetic parameters (from experimental data, theoretical principles) for the surface elementary steps (including adsorption, desorption, Langmuir-Hinshelwood steps, *etc*.) involved in a proposed possible mechanism of the reaction [53]. More and more utilizations of this powerful method are found in the literature. Weber *et al.* [54] adopted a “building up” strategy to construct a microkinetic model for complex systems, in which the overall reaction network is built from several sets of basic reactions that are as independent as possible (i. e., share as few intermediates as possible) and that are consistent with the known chemistry of surface species. The DETCHEM package [6] was developed employing a similar approach. Deutschmann *et al.* [55]developed the mechanism for catalytic methane partial oxidation on a rhodium catalyst. In simulating a TWC of Pt/Rh, Chatterjee *et al.* [56] developed a mechanism for the possible reactions of CO and NO on rhodium. These studies are the bases for the mechanism development presented in this study.

3.3.3 Determination of Arrhenius kinetic parameters

It is generally very difficult to determine the key reaction rate coefficients, i.e. the initial adsorption coefficients, the activation energies of surface reactions, and the temperature exponential (referring to *kinetic data* in this thesis, see Tables in the Appendices). The reason for this difficulty is on the one hand that there are mostly a very huge number of elementary reaction steps, and is on the other hand that most coefficients are temperature dependent.

A detailed description of the complex reaction mechanisms, or complete mechanism often results in a large number of reaction steps, and hence a large number of Arrhenius kinetic parameters to be determined. Since, as described above, it is too time-consuming to determine all kinetic parameters experimentally, alternative approaches have to be taken instead.

In her dissertation [57], Olsson summarized a list of methods to determine the rate parameters in the kinetic model: (1) Literature values; (2) Thermodynamic restrictions, (3) Collision theory, (4) Statistical thermodynamics, (5) Transition state theory, (6) Regression analysis and (7) Quantum chemical methods such as density functional theory calculations. All of these approaches are utilized in this study.

Although the fundamental theoretical calculations, e.g. first principle ab-initio methods, and density function theory (DFT), are increasingly available, their application to complex reaction systems and their generalization to practical catalysts are still beyond the current available computational capacities. They are however frequently used for the calculation of heats of adsorption.

3.3.4 UBI-QEP approach to calculating the reaction energies

Since 1980's, Shustorovich *et al.* have developed a semi-empirical method, which is called bond-order conservation-Morse-potential method (BOC-MP) [7] and recently has been generalized to unity bond index-quadratic exponential potential (UBI-QEP) [8], to calculate the reaction energetics (heats of adsorption, reaction enthalpy and activation barriers) at varied coverages. This method first calculates the heats of adsorption with the gaseous bond dissociation energies as the input, and then calculates the activation energies in a thermodynamically consistent way. Most importantly, UBI-QEP can predict the coverage dependence effects on the energies. In the latest comprehensive review [8], Shustorovich and

Sellers stressed that phenomenological modeling in general and the UBI-QEP modeling in particular is not competitive with but complementary to quantum mechanical modeling. In addition, in practice, they showed how the two approaches can be synergistically combined. The theoretical method usually can supply the necessary small molecules' heats of adsorption for the input of UBI-QEP calculation. More recently, Sellers *et al.* combined the two methods of DFT and UBI-QEP to construct the whole mechanism by using the ab-initio calculations to calculate the reaction rate preexponentials (though very difficult to do this), and using UBI-QEP to calculate the activation energies [58].

The fundamentals of the UBI-QEP (BOC-MP) approach are omitted here, since they are well documented in the literature [7, 8].

3.3.5 Heats of adsorption values

It is necessary to know the heat of adsorption for molecular species are the first step to build up the elementary surface reaction mechanism. This can be achieved in two ways. If isosteric heats of adsorption from literature are available, then those values are preferred. In other case, the heat of adsorption may be approximated by the activation energy for desorption, since normally molecular adsorption is regarded as a non-activated process [59]. Crystallographic orientation is known to have an influence on the heat of adsorption, yet this effect is thought to be of secondary importance. Hence, the values for enthalpy of adsorption have been chosen for close packed planes. Another complication is that the heats of adsorption (for both molecular and dissociative adsorption) also vary with adsorbates' coverages on the surface due to lateral interactions. In the field of mean-field approximation, these effects have been neglected or counted in a way that assuming the activation energy has linear dependence with the related adsorbates' coverages. Therefore, only heats of adsorption at low coverage, where lateral interactions are negligible, are normally collected [60].

Based on the idea mentioned above, heats of adsorption of small molecules are collected from literature for the construction of the detailed mechanism for the DeNO$_x$ system. Clearly, these are very important, as C, H, O and N (even S) are the principle building blocks of most of the species involved in the fundamental processes of heterogeneous catalysis for related research topics.

3.3.6 Adsorption and binding geometry

The possible adsorbing and binding geometry for the NO-O_2 on Rh(111) surface is shown in Figure 3-4. Another example for possible adsorption species during propene oxidation over rhodium is shown later in Figure 3-5. These are very important for calculating the adsorption energies and activation energies using the UBI-QEP approach.

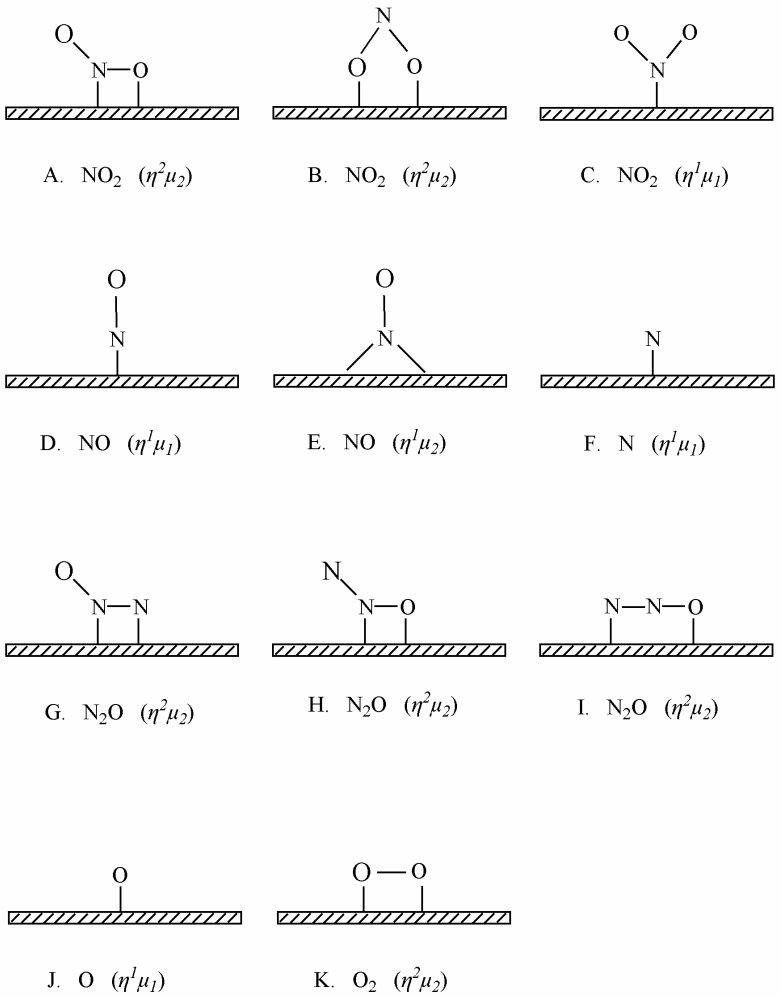

Figure 3-4 Schematic illustration of possible adsorption sites of NO_2, NO, and O_2 for NO-O_2 system on Rh(111) surface. Note: where, coordination type, η^i-coordinating-atom surface species (connecting with surface Rh) with the number of i, and μ_j -coordinating Rh metal atom with the number of j.

3.4 Reaction mechanism over rhodium

3.4.1 Introduction

The successful specific design of catalytic converters for specific applications requires an accurate comprehension of the involved surface reactions and transitions.

Not only have these transition to be understood under steady-state conditions, but also and presumably more importantly under transient conditions. Most currently available models of the kinetics are valid only under steady-state conditions and cannot adequately describe the dynamic effects of rapid changes of reaction conditions. Moreover, another limitation of the available models is that they are usually specific to a given catalyst. That is, one has to adapt at least a minor number of parameters or even reaction pathways to properly simulate another similar reaction system which is only little different from the previously studied system. Thus, an accurate kinetic model that can account for different conditions is very desirable.

This study is a considerable step in the direction of this target. We follow the above-mentioned approach and develop a complete mechanism for the entire studied system, step by step. The phenomenological UBI-QEP method is taken to calculate the heats of chemisorption, the reaction enthalpies and the reaction activation energies for several elementary reaction networks for CO-O_2, H_2-O_2, NO-O_2, and C_3H_6-O_2 systems over rhodium. The full mechanism used in the simulation is listed in Appendix Table A-1.

3.4.2 CO oxidation

The mechanism for CO oxidation over Rh (hereafter, called CO-O_2 system) is divided into several subsystems,

(1) Oxygen adsorption and desorption,
(2) CO adsorption and desorption,
(3) CO_{ads} and O_{ads} combination into CO_2 through the Langmuir-Hinshellwood (L-H) mechanism, in which reactions happen between the adsorbed species,

where subscript ads denotes adsorbed species on Rh surface.

3.4.3 H_2 oxidation

The mechanism for H_2 oxidation over Rh (hereafter, called H_2-O_2 system) is also divided into several subsystems,

(1) Oxygen adsorption and desorption (in common with the CO-O_2 system),
(2) Hydrogen adsorption and desorption,
(3) Water adsorption and desorption,
(4) OH adsorption and desorption,
(5) H_2O_{ads} decomposition into H_{ads} and OH_{ads},
(6) OH_{ads} and H_{ads} combination into H_2O_{ads} through the L-H mechanism,
(7) OH_{ads} and OH_{ads} recombination into H_2O_{ads} and O_{ads} through the L-H mechanism,

3.4.4 NO reduction and oxidation

The mechanism for NO decomposition over Rh (hereafter, called NO-O_2 system) is divided into the subsystems,

(1) Oxygen adsorption and desorption (in common with the CO-O_2 system),
(2) NO adsorption and desorption,
(3) Dissociation of NO_{ads} into surface N_{ads} and O_{ads},
(4) N_2O adsorption and desorption,
(5) Two adjacent N_{ads} recombination to N_2,
(6) N_{ads} and NO_{ads} recombination into N_2O_{ads},
(7) NO_2 adsorption and desorption (only considered for NO-O_2-NO_2 system example in this work),
(8) NO_{ads} and O_{ads} recombination into $NO_{2,ads}$ (only considered for NO-O_2-NO_2 system example in this work).

It is worth noting that in the N_2 formation mechanism, according to [61], two pathways (direct and indirect) are assumed. In the direct pathway, two adjacent surface N species combine into N_2, and in the indirect pathway, N_2O is assumed as intermediate to N_2 formation during the NO decomposition:

Surface N_2O formation:

$$N_{ads} + NO_{ads} \rightarrow N_2O_{ads} + Rh_{ads}. \quad 3.6$$

β-N_2 Mechanism (direct N_2 formation):

$$N_{ads} + N_{ads} \rightarrow N_2 + 2Rh_{ads} \quad 3.7$$

δ-N_2 Mechanism (N_2 formation through N_2O route):

$$N_2O_{ads} \rightarrow N_2 + O_{ads}. \quad 3.8$$

$$N_2O_{ads} \rightarrow N_2O + Rh_{ads}. \quad 3.9$$

where Rh_{ads} denotes the vacant Rh site.

Therefore, the way to decrease the N_2O content from the exhaust is either minimizing its production during the NO decomposition process or catalytic decomposition of the N_2O after being produced during the earlier process. There are several papers reporting the catalytic decomposition of N_2O over supported or single crystalline Rh catalysts [62]. For example, Zeigarnik reviewed the data on the interaction of nitrous oxide with polycrystalline and low-index single crystal surfaces of transition metals (Cu, Ag, Pt, Pd, Ni, W, Ir, Rh and Ru) in a recent paper [63]. Yet, the mechanism of N_2O production and reduction is still uncertain. Here we presented an approach with the UBI-QEP approach to calculate the energetics (activation energies) of the N_2O related mechanism. The kinetics of N_2O adsorption, desorption, and dissociation on these surfaces, as well as the reaction pathways of these processes, are considered. New calculated data on the energetics of nitrous oxide transformations on Rh(111) single crystalline transition metal surfaces are reported in this thesis. We also evaluated the importance of the value of the adsorption energy of N_2O to the simulation results of NO decomposition by comparing different values (Refer to Chapter 4). It shows the importance of the N_2O mechanism in the NO decomposition modeling.

3.4.5 C_3H_6 oxidation

A rather simple mechanism is studied for simulation of propene oxidation in presence of oxygen and in presence of oxygen and NO over Rh by analogy with C_3H_6 on Pt [56].

Stepwise mechanism: In this mechanism, the reaction was supposed to be stepwise H abstraction quasi-elementary reactions, which is not according to the experiments:

$$C_3H_6 + Rh_{ads} \rightarrow C_3H_{6,ads} \quad ,$$
$$C_3H_{6,ads} + Rh_{ads} \rightarrow C_3H_{5,ads} + H_{ads} \quad ,$$
$$C_3H_{5,ads} + Rh_{ads} \rightarrow C_2H_{4,ads} + CH_{ads} \quad ,$$
$$C_2H_{4,ads} + Rh_{ads} \rightarrow CH_{2,ads} + CH_{2,ads} \quad ,$$
$$CH_{2,ads} + Rh_{ads} \rightarrow CH_{(s)} + H_{ads} \quad ,$$
$$CH_{ads} + O_{ads} \rightarrow CO_{ads} + H_{ads} \quad ,$$
$$\ldots$$

However, no kinetic data are given in [64].

Detailed mechanism: In a pioneering study [65], Yao conducted a detailed study on the oxidation of CO and hydrocarbon (propene, 1-hexene and toluene) on unsupported wires or supported noble metal (Pt, Pd or Rh). It was proposed (also from the comparison with the saturated hydrocarbons [66]) that the adsorption of the hydrocarbon double-bond adsorption and breaking could be rate controlling. By analogy with C_3H_6 on Pt [56], two routes for propene adsorption are considered:

- C_3H_6 direct adsorption on Rh surface

$CH_2{=}CHCH_3 + 2Rh_{(s)} \rightarrow CH_3\text{-}CHCH_{2\,(s)}$ $(\eta^2\mu_2)$ (see Figure 3-5 (B));

- O aided H abstraction and produce propenyl ($CH_2{=}CHCH_2$-Rh) and $OH_{(s)}$

$CH_2{=}CHCH_3 + O_{(s)} + Rh_{(s)} \rightarrow OH_{(s)} + CH_2{=}CHCH_{2,(s)}$ $(\eta^1\mu_1)$ (see Figure 3-5 (F)),

where, coordination type: η^i-coordinating-atom surface species (connecting with surface Rh) with the number of i, and μ_j- coordinating Rh metal atoms with the number of j. The suggested adsorption species and possible intermediates structures for propene on Rh are illustrated in Figure 3-5.

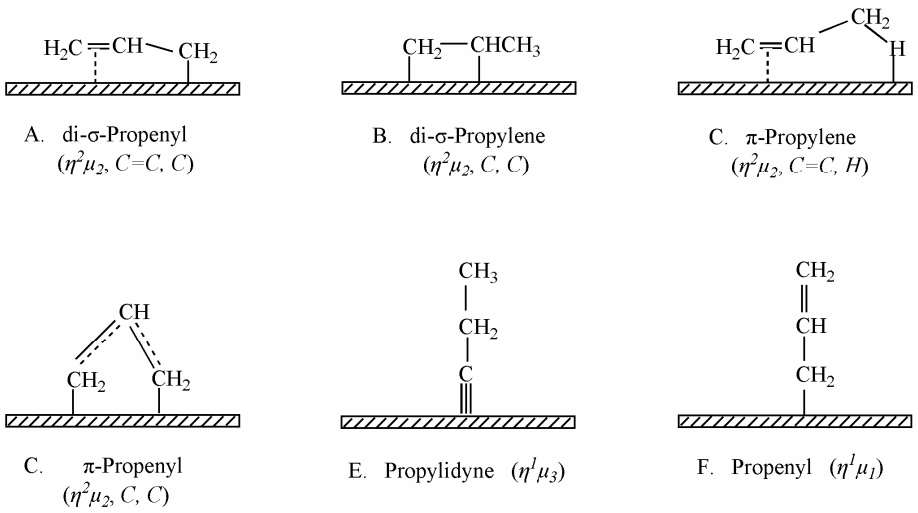

Figure 3-5 Schematic illustration of possible adsorption sites and intermediates for propene on Rh(111) surface. Note: where, coordination type, η^i-coordinating-atom surface species (connecting with Rh) with the number of i, and μ_j -coordinating Rh metal atom with the number of j.

Chapter 4: Transient Simulation of Reduction of NO by CO or H_2 in the Presence of Excess Oxygen over Rhodium

In this chapter, the simulation results for the transient catalytic NO_x decomposition system is presented based on the microkinetic model developed in the preceding chapter. The reductant used in this study is CO or H_2. The mechanism of the NO decomposition is discussed.

4.1 Introduction

4.1.1 Background

Although it has long been demonstrated that both CO and H_2 participate in the reduction of NO_x [67], they have not been thought of as efficient and selective reductants until recently, since CO and H_2 are mostly oxidized by oxygen rather than by NO under lean conditions. However, recent studies have shown that in addition to hydrocarbons, CO and hydrogen have proven to be effective for NO reduction under lean (oxygen-rich) conditions. Moreover, improving the low-temperature activity of the catalyst is necessary and crucial for the

automotive start-up (cold-start) to meet stringent regulations. Consequently, a catalyst, that is able to effectively reduce NO_x to N_2 (rather than to N_2O) using CO, H_2 or C_3H_6 as the reductant at low temperature, is highly desired.

In this chapter, CO and H_2 were used as reductants for NO_x decomposition/reduction over a rhodium based catalyst operated under periodic lean/rich cycles in order to study the feasibility of CO/H_2-SCR/$DeNO_x$.

4.1.2 Motivation

In order to verify whether the DETCHEM module-DETCHEM^{TRANSIENT}, parallely developed by Inderwildi *et al.* [5] within the ConNeCat project, could indeed catch the features and predict the transient behavior of a monolithic catalyst, the parameter study was conducted. Then a comparative study between measurements of transient conversions in a monolithic catalyst loaded with rhodium and transient simulation of such a system was performed to study the kinetic behavior of the catalytic system proposed by Nakatsuji [3, 68, 26, 69].

Due to the well-known importance in the field of automotive exhaust gas catalytic purification, the kinetics of CO oxidation reaction as well as CO-NO reaction in the presence or absence of O_2 over rhodium system has been studied intensively in the last decades [70, 71]. As a result, the mechanism of the above reaction systems for the steady-state is available and also well benchmarked [72]. Therefore, in the first comparative study, the simulations with DETCHEM^{TRANSIENT} and transient measurement of conversions over a rhodium-based monolithic catalyst were carried out using CO as reductant.

However, one has to bear in mind that it is difficult to investigate experimentally the reduction of NO_x with CO. Because CO and N_2 have the same molecular mass, hence, to monitor the formation of nitrogen by means of mass spectrometry, either a reductant with isotopically labelled carbon (e.g., ^{13}C) [73] or a carbon free reductant has to be utilized, or using isotopically labelled nitrogen (e.g., ^{15}N) [73] to substitute ^{14}N for NO. Otherwise, one could not distinguish the overlapping mass peaks of CO and N_2. Furthermore, the products of CO-NO reactions, CO_2 and N_2O also have same molecular mass. Moreover, since labeled compounds (^{13}CO or ^{15}NO) are very expensive and therefore they are not economic and applicable for transient flow measurement. The N_2 production is deduced from the equation as given below:

$$X_{N_2} = \frac{X_{NO,inlet} - X_{NO,outlet} - 2 \times X_{N_2O,outlet}}{2}.$$

Owing to these reasons, further detailed transient mechanistic and comparative study was conducted with H_2, a carbon-free reductant.

4.2 Parameter study

4.2.1 Introduction

In this section, a parameter study is done at the initial stage of the ConNeCat project. The goal is to check the feasibility of the available mechanism and to decide some important parameters.

Throughout the thesis, the stoichiometry number *S* is defined for characterizing the air-fuel-ratio (AFR) as:

$$S = \frac{2X_{O_2} + X_{NO}}{X_{CO} + X_{H_2} + 9X_{C_3H_6}}, \qquad 4.1$$

where, $S > 1$, $S = 1$ and $S < 1$ indicates lean, stoichiometric and rich condition for the simulated exhaust gas respectively. The selectivity of N_2 is defined as the percentage of the produced N_2 concentration in the total products from NO conversion (here in this work means mainly the production of N_2 and N_2O, neglecting other nitrogen containing species such as NH_3):

$$S_{N_2} = \frac{X_{N_2}}{X_{N_2} + X_{N_2O}} \times 100\% \qquad 4.2$$

The CO-O_2-NO system was simulated with DETCHEM^{TRANSIENT} code. To study the effect of O_2 concentration, and thus the effect of the stoichiometry number S on the CO and NO conversions, two simulations of parameter study were conducted.

4.2.2 Effect of O_2 concentration during the rich period

In this study, the simulation was performed by varying O_2 concentrations during the rich period while keeping the other conditions constant.

The oxygen concentration was varied from 6% to X% (note X=0.975 corresponds to the stoichiometric condition) in order to simulate the lean/rich periods in the experiments. A uniform single channel inlet velocity of 1.0 m/s is used to simulate the exhaust gas flow.

The simulation conditions were as follows:

Lean: 2% CO, 500 ppm NO, 6% O_2 in argon (Ar);

Rich: 2% CO, 500 ppm NO, X% (X = 0.1-10) O_2 in Ar;

Lean/rich span: 2 cycles 2 s/0.2 s;

Temperature: 600 K.

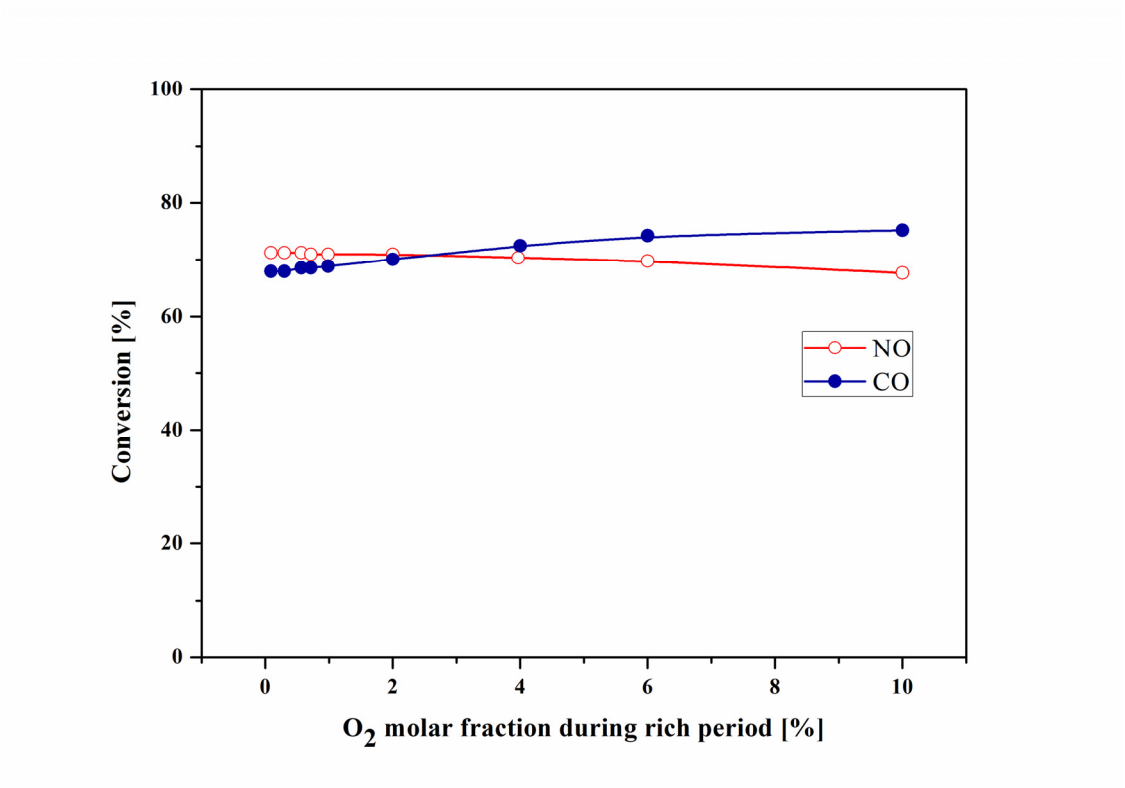

Figure 4-1 Effect of O_2 during rich period on the transient CO and NO conversions, see text for explanation. Reaction conditions: T=600 K; Lean: CO=2.0%, NO=500 ppm, O_2=6%, filling gas Ar; Rich: CO=2.0%, NO=500 ppm, O_2= X% (X=0.1-10), filling gas Ar.

Figure 4-1 displays the simulation results of the CO and NO conversions. It shows that there is no significant influence resulting from varying the O_2 concentrations during the short rich period. The results give important clues for the experiments, which are conducted for the validation of the model developed in this thesis. Therefore, in the subsequent experimental study (see chapter 4.4), the O_2 concentration in the rich period is taken as zero for the ease of realizing the lean/rich spans by turning on/off the Mass Flow Controller (MFC) only.

4.2.3 Effect of O_2 concentration during the lean period

With varying O_2 concentrations X% (X= 0.1-6) during the "lean" periods (2 s) while taking the constant O_2 concentration of 0.9% during the rich period (0.2 s), the simulation of the transient CO and NO conversions was performed. The other conditions are the same as the above study for Figure 4-1. The results are shown in Figure 4-2. Drastic increases can be seen for the CO oxidation and also decreases for NO conversion were observed.

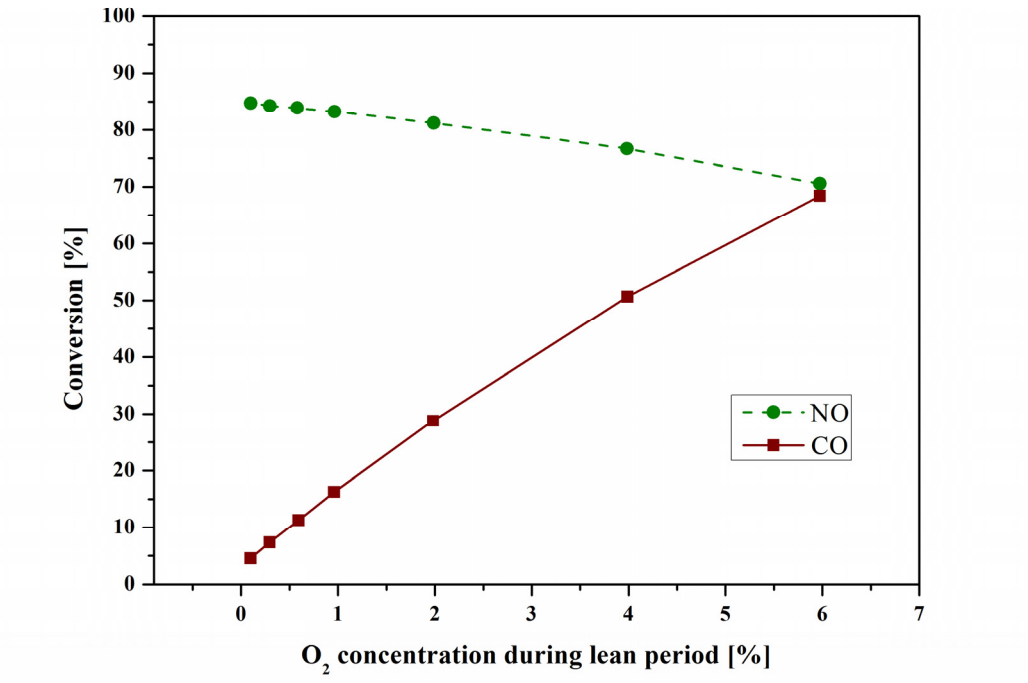

Figure 4-2 Effect of O_2 during lean period on the transient CO and NO conversions, see text for explanation. Reaction conditions: T=600 K; Lean: CO=2.0%, NO=500 ppm, O_2=X% (X=0.1-6), filling gas Ar; Rich: CO=2.0%, NO=500 ppm, O_2=0.9%, filling gas Ar.

4.2.4 Light-off performance of the simulated system

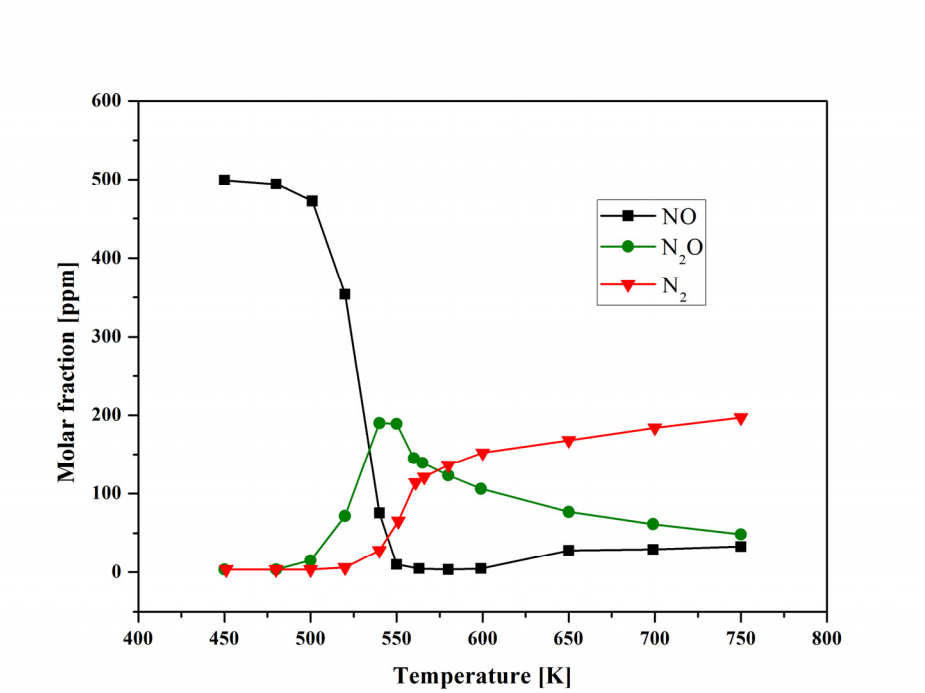

(a)

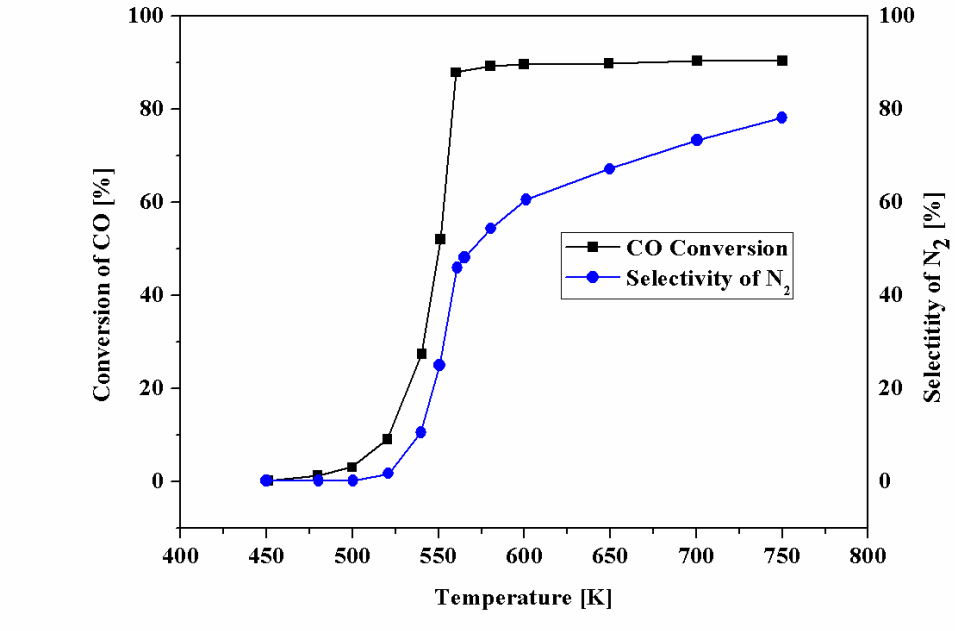

(b)

Figure 4-3 Light-off curves for the CO-NO-O_2 system (simulation results). (a) NO, N_2O, N_2 concentrations vs. Temperature; (b) CO conversion and N_2 selectivity vs. temperature. Lean: CO=5.0%, NO=500 ppm, O_2=8%, filling gas Ar; Rich: CO=5.0%, NO=500 ppm, O_2=0.8%, filling gas Ar.

Figure 4-3 shows the light-off curves for the CO-NO-O_2 system. It can be found that the concentration of NO first decreases with the temperature to a minimum at about 550 K, and then keeping almost invariable until 750 K, except for a minor increases above 600 K. This may be due to the increases of NO molecular desorption at higher temperature. At the same time, the concentration of N_2 steadily increases with the temperature and exceeds that of N_2O at around 570 K, i.e. the selectivity of N_2 exceeds 50%.

4.2.5 Comparison of transient and stationary performances

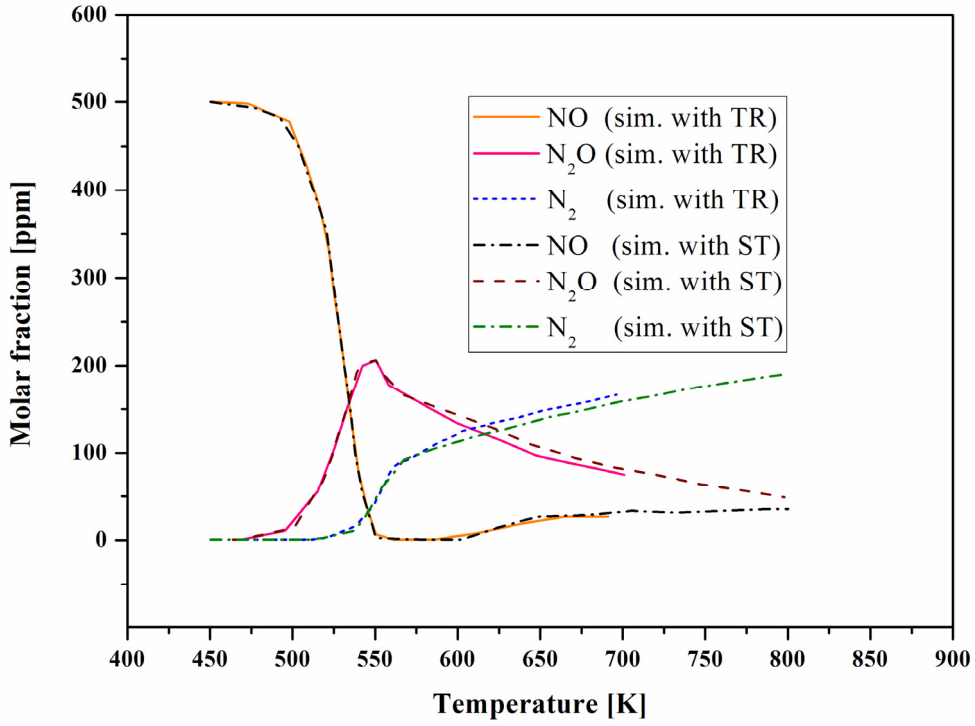

Figure 4-4 Comparison of the simulation of the transient (with DETCHEM^{TRANSIENT}) and the steady-state performances (with DETCHEM^{CHANNEL}). Transient conditions, 2 cycles lean/rich= 1 s/0.1 s, Lean: CO=5%, NO=500 ppm, O_2=8.0%, fill Ar, Rich: CO=5%, NO=500 ppm, O_2=0.8%, fill Ar; stationary conditions, CO=5%, NO=500 ppm, O_2=8.0%.

To study the effects of the short rich periods on the NO_x reduction during the lean-rich-cycle system, a series of simulations were conducted with DETCHEM^{TRANSIENT} and DETCHEM^{CHANNEL} for transient conditions and stationary conditions, respectively. From Figure 4-4, it can be seen that the difference is minor between the simulation results from the transient and the stationary simulation, which is contradictory to the experimental results. The

minor difference is checked to be mainly caused by the difference of stoichiometric number in the two cases. That is to say, with this available mechanism describing steady-state kinetics, it could not simulate/catch the transient features brought by the transient lean/rich cycles as Nakatsuji et al. reported [3, 26]. From the comparison results, it seems that the short rich period has nearly no effects on the NO conversion. The main role of the short rich period may be the resistance to SO_x ageing referring to previous work done by Nakatsuji et al. [3, 26].

The results may call for a more comprehensive and reasonable mechanism to account for the discrepancy between this initial simulation and the experimental results under lean/rich transient conditions. Therefore, the central task is to make an effort towards this target within the content of this thesis.

4.2.6 Effect of the kinetic data for N_2O desorption on the N_2 selectivity

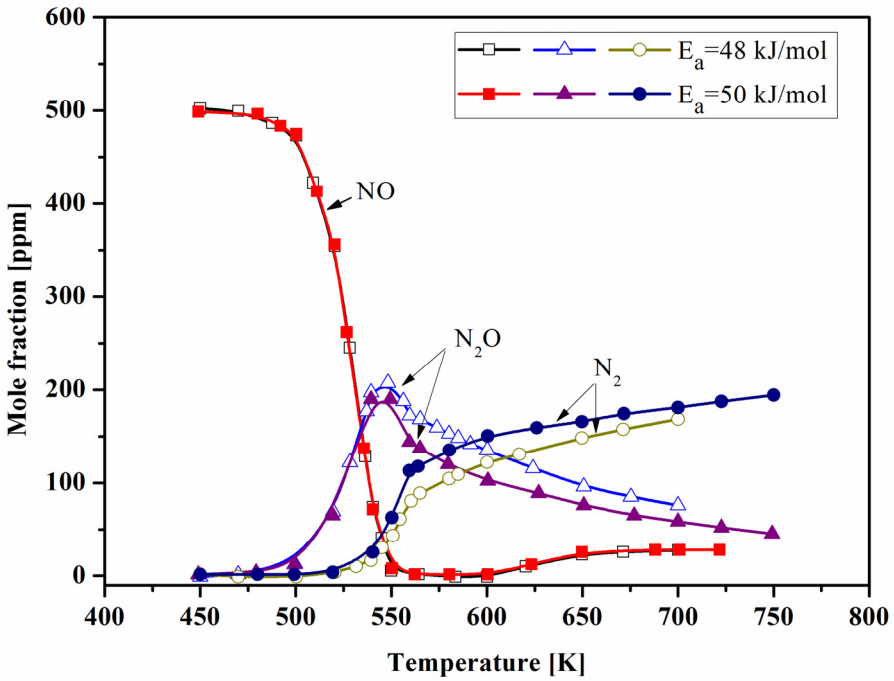

Figure 4-5 Crucial effect of the activation energy (E_a) of N_2O desorption for predicting light-off curves for the CO-NO-O_2 reactions. Simulation conditions: Lean: CO=5.0%, NO=500 ppm, O_2=8%, filling gas Ar; Rich: CO=5.0%, NO=500 ppm, O_2=0.8%, filling gas Ar.

Further simulation was conducted as another example for parameter studies which uses different activation energies E_a for N_2O desorption, and gave some clues to the detailed

mechanism to be used for the $DeNO_x$ system modeling, cf. Chapter 3 for mechanism details. In the literatures, no accurate kinetic data on N_2O formation and decomposition mechanism are available. This reflects the situation of the research on this topic: the contradictory conclusions on the existence of N_2O (in the early days) and its mechanism in the course of the NO decomposition can be found. Some authors claimed that N_2O were not observed in their experiment [72], while the others are entirely opposite [74, 75]. Results in Figure 4-5 show clearly that the value of E_a plays a crucial role in the modeling of NO decomposition kinetics, especially for the selectivity of N_2.

4.2.7 C_3H_6-O_2–NO reaction

In this study, the simulation was performed to study the propene oxidation and NO reduction. The situation is that there are very few data (theoretical or experimental) concerning the hydrocarbon (C_xH_y, $x\geq2$) oxidation mechanism on the Rh surface, because Rh is thought of as mainly a good reduction catalyst but not a good oxidation catalyst, and furthermore its content is much less than the other noble metal (Pt, Pd, *etc.*) in the catalyst used in the TWC or $DeNO_x$ catalysts. Normally only the CO oxidation and NO reduction as well as oxidation processes are considered for the Rh surface, omitting the kinetics of HC oxidation on the Rh surface [56]. For the HC aided Selective Catalytic Reduction of NO_x (HC-SCR) reported in the literature, Rh is normally present in combination with Pt in the catalyst, so it is not easy to explicitly validate the supposed propene oxidation mechanism over Rh.

When the initial study was conducted, neither stationary nor transient experimental results were available from our partners Umicore and hte-company within ConNeCat project. Therefore, some related research results from literatures to validate the initial propene oxidation mechanism on the Rh surface. Nikolopoulos, Efthimiadis and their coworkers conducted a series of experiments on selective reduction of NO by propene in the lean conditions on Pt- and Rh-supported alumina catalysts [76, 77].

Experimental [76, 77] The catalyst used was Rh/γ-alumina prepared with the incipient wetness method. The actual Rh loading was measured by induced coupled plasma and atomic emission spectroscopy (ICP/AES) and was found to be 1.86±0.05 wt.%. The dispersion of Rh atoms was about 60% by H_2 chemisorption studies assuming the surface H:Rh ratio was unity. The overall pore volume of the catalyst was 0.5 cm^3/g, with mercury porosimetry measurements. The pore diameters varied mainly in the range of 0.005–0.02 μm. The catalyst

weight used in the experimental was 0.15 g. The experimental conditions were as follows [76]: 1000 ppm propene (C_3H_6), 5.0% O_2, fill He; fixed-bed reactor, Rh/alumina, W/F=0.018 g·s/cm^3.

The simulation results are shown in Figure 4-6. For the propene oxidation without NO, the light-off curve is simulated quite well in the tendency. However, in presence of 1000 ppm NO, the simulation can not predict the strong inhibition effect from the addition of NO as in the experiments. This may reflect the limitation of the simple mechanism used for the simulation.

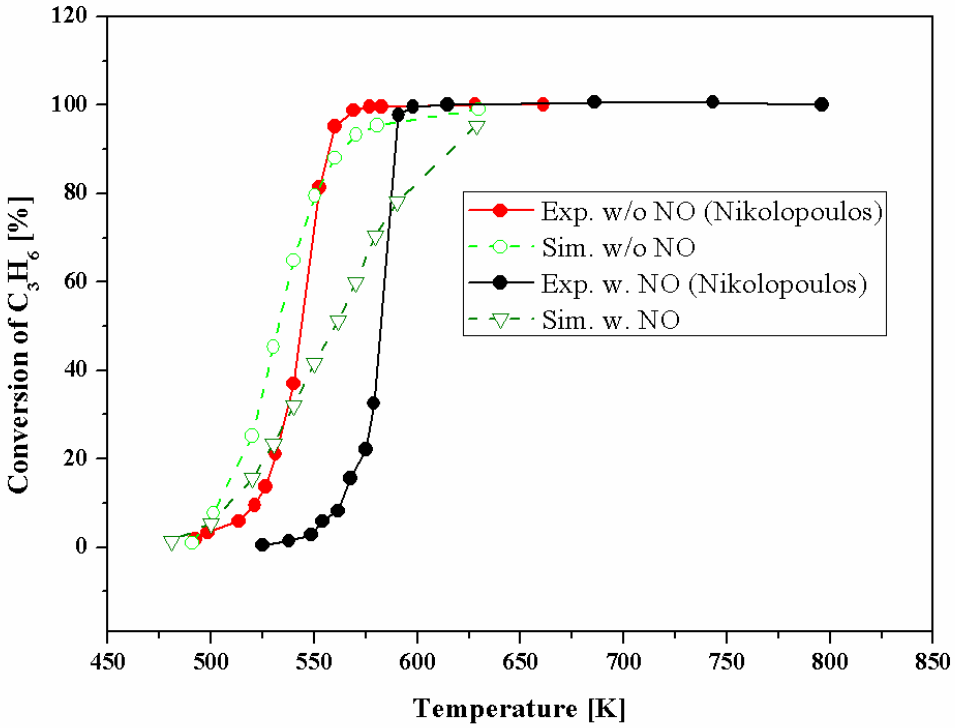

Figure 4-6 Light-off curves for the C_3H_6-O_2 in the absence and in the presence of over Rh catalyst. Conditions: C_3H_6=1000ppm, O_2=5%, NO=0 ppm or1000 ppm, fill He. In the caption, w/o means “without” and w/ means “with”.

4.3 Simulation of a single channel of monolith reactor

4.3.1 Experiments for the simulation

A series of experiments on NOx reduction by CO or H_2 under alternating lean/rich condition in a laboratory-scale tube reactor were conducted by the project partner, hte-Company[4]. A rhodium-loaded monolithic catalyst was used in the experiments. For testing in the lean/rich cycles, a core of 3x3 channels was applied. The experiments were performed with the instruments described in Table 4-1.

The oxygen concentration was varied from 8% (14.5%) to 0% in order to simulate the lean/rich periods during the experiment, while the concentration of NO and the reducing agent was kept constant. The volume flow rate of the gas mixture in the reactor was 30 l/h at standard conditions (25 °C). A uniform superficial velocity of 0.926 m/s corresponds to this volumetric flow. The catalyst's characteristics are listed in Table 4-2.

Table 4-1 Experimental Techniques

Analytic Tool	Model	Manufacturer
FT-IR spectrometer	Protégé 460	Nicolet
Mass spectrometer (Quadrupole)	QMG 422	Pfeiffer
Lambda sensor	LSU 4.2	Bosch
Nitrogen oxide analyser	CLD 700 EL ht	Ecophysics

Table 4-2 Catalyst parameters used in the numerical simulation of the $DeNO_x$ catalyst

Washcoat loading	210 g/l
Number of channels of the monolith reactor	9
Noble metal loading	0.3 mg
Active noble metal surface	0.80 m^2/g

[4] The measurements were done by Dipl. -Ing. Jürgen Maier, hte-Company, Heidelberg.

(determined by CO chemisorption)	
$F_{cat/geo}$ (Catalytic surface/geometric surface)	110
Channel diameter	1 mm
Channel length	30 mm
Superficial velocity (STP)	0.926 m/s

The experimental conditions for CO oxidation by O_2 in the presence and absence of NO were listed in Table 4-3.

Table 4-3 Experimental conditions

Reaction condition	CO		H_2	
Lean/rich period	60 s/5 s		60 s/5 s or 60 s/2 s	
Investigated temperature	165-425 °C		165-425 °C	
	Lean	Rich	Lean	Rich
H_2	-	-	2%	2%
CO	0.5%	0.5%	-	-
NO	500 ppm	500 ppm	500 ppm	500 ppm
O_2	8.0%	0%	14.5%	0%
N_2	Balance	Balance	Balance	Balance

4.3.2 CO-O_2 reactions over rhodium

The simple CO-O_2 reactions over rhodium were taken for the first comparative study to investigate the transient conversion of the catalytic system using the detailed mechanism developed in Chapter 3. This system was studied with a lean phase of 60 s and rich phase of 5s.

The results for the CO conversion as a function of the temperature determined experimentally and theoretically are shown in Figure 4-7. The simulation results clearly show that the light-off temperature, at which 50% conversion achieved, is about 200 °C. Above 205 °C, the simulation predicts a nearly constant CO conversion. Above 250 °C the simulation underestimates the CO conversion by within 8%. This discrepancy in CO conversion at higher temperature might be understood in a way that the mechanism used for simulation accounts for higher CO desorption due to higher (constant) adsorbates' interactions.

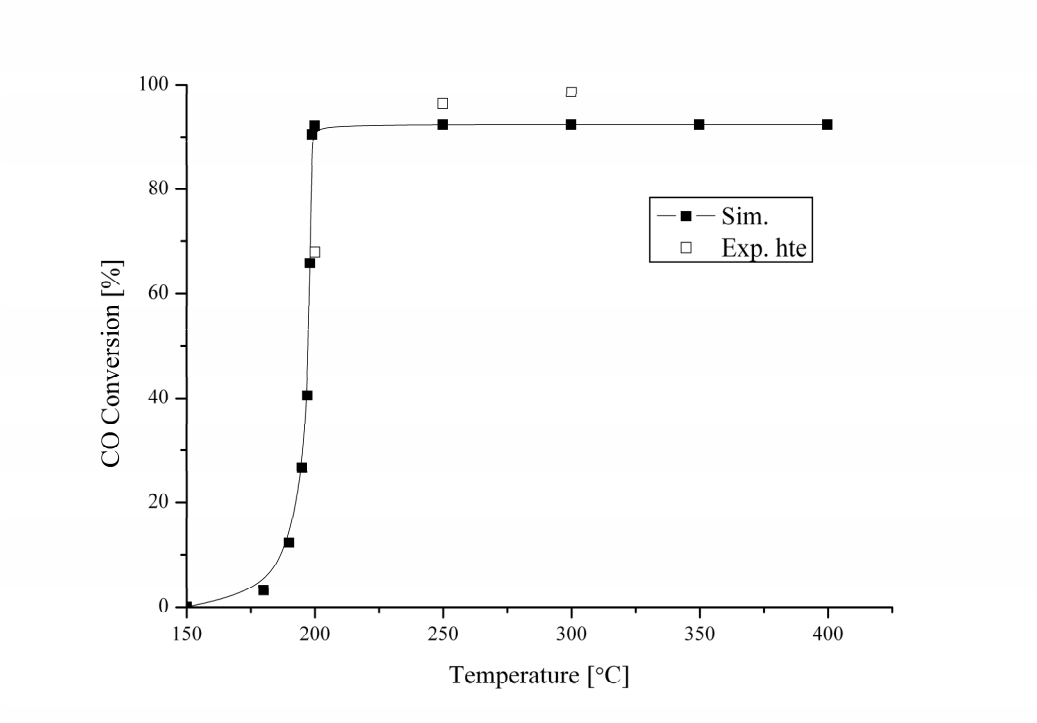

Figure 4-7 CO conversion vs. temperature–a light-off curve. Conditions: Lean/rich: 60 s/5 s, Lean: CO=0.5%, O_2=8%, fill N_2; Rich: CO=0.5%, fill N_2.

4.3.3 CO-O_2-NO reactions over rhodium

To study the possible reducing ability of CO on NO_x over rhodium catalyst, a simulation study was conducted for the CO-NO-O_2 reaction system with DETCHEM^{TRANSIENT}.

The average mole fraction of the outlet NO versus temperature was simulated and the results were compared with experimentally determined conversions (Figure 4-8(a)). As can be

seen from Figure 4-8(a), the nitrogen oxides were converted selectively to N_2 (as high as 97%). The agreement between the experimentally determined value and the theoretically predicted one is adequate in both trend and absolute values. These results reflect the expected poorer reducing performance of CO: above 250 °C only less than 50 ppm NO are converted, while in case of hydrogen 200 ppm are converted, see 4.3.4.

The results for the CO conversion as a function of the temperature as determined experimentally and theoretically are demonstrated in Figure 4-8(b). The simulation determines the light-off temperature to be at 270 °C. The simulation results predict a nearly constant CO conversion above 275 °C, and underestimate the CO conversion by within 8% above 350 °C.

It is interesting to point out the role of the addition of NO into the CO-O_2 reaction. Comparing the results for the CO-O_2 reaction in absence of NO (Figure 4-7) with that in presence of NO (Figure 4-8(a)), the former system shows much lower light-off temperature than the latter one (200 °C *vs*. 265 °C). This indicates that the addition of NO has a strong inhibition effect on the CO oxidation. It has already been noted and stressed by Oh *et al*. [78] that similar effects exist over a Rh/Al_2O_3 catalyst under steady-state conditions. In that study, this strong inhibition effect was reasonably explained on the basis of a mechanism involving the blocking of the reactive sites by molecularly adsorbed NO [78]. This mechanism also interprets the much weaker effect over alumina-supported platinum catalyst, whose surface is supposed to be dominated by the adsorbed CO in the case of CO-NO-O_2 reaction system, whereas adsorbed NO on the supported rhodium surface. Here under transient conditions, where the rhodium surface is mainly covered by O(s), it seems that the same mechanism could explain the similar effect.

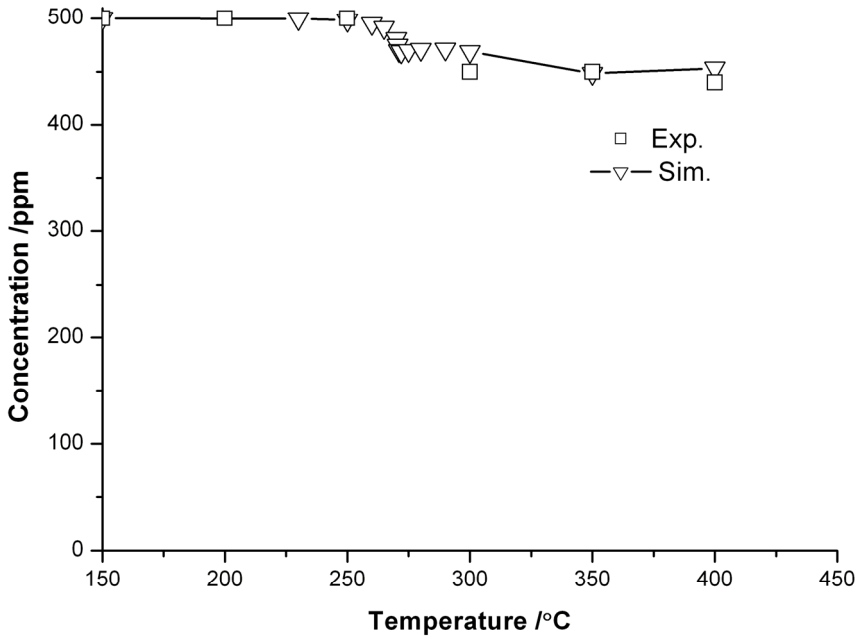

(a)

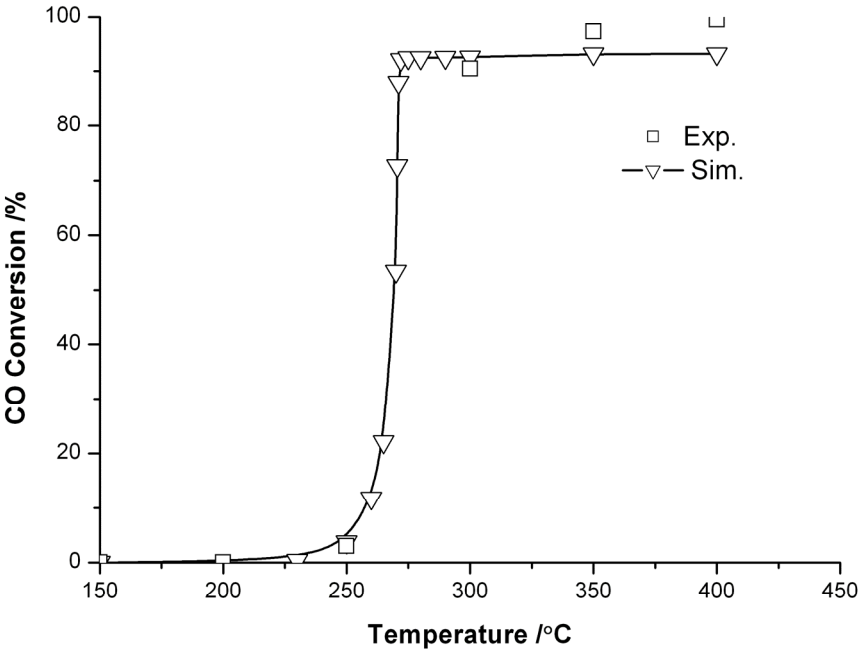

(b)

Figure 4-8 Conversion curves with the transient lean/rich period (a) Mean outlet NO concentration versus temperature; (b) Conversion of CO. Conditions: Lean/rich: 60 s/5 s, Lean: CO=0.5%, O_2=8%, NO=500 ppm, fill N_2; Rich: CO=0.5%, NO=500 ppm, fill N_2.

4.3.4 H_2-O_2-NO over rhodium

In order to study the impact of a different reductant, an analogous system with H_2 instead of CO was studied. The results of simulations are compared to experimental observations. The NO_x reduction with hydrogen was simulated with DETCHEM^{TRANSIENT}: two different lean/rich periods, 60 s/5 s and 60 s/2 s, were studied. The temperature dependence of the NO conversion and the influence of different lean/rich period ratios are discussed.

Temperature dependence of the transient NO conversion behavior

The average concentration of NO in the outlet gas versus temperature in the 60 s/5 s (lean: 60 s, rich: 5 s) system is simulated with DETCHEM^{TRANSIENT} and the results are compared with experimental results, as shown in Figure 4-9. Both investigations - theoretical and experimental - clearly show that, the NO concentration decreases to a minimum at around 200 °C, with a maximum NO conversion of 57%. Above 200 °C the NO concentration increases with increasing temperature. Having in mind that the actual noble metal loading is just 0.3 mg, *i.e.* 0.25% of the catalyst weight, this conversion is extraordinarily high.

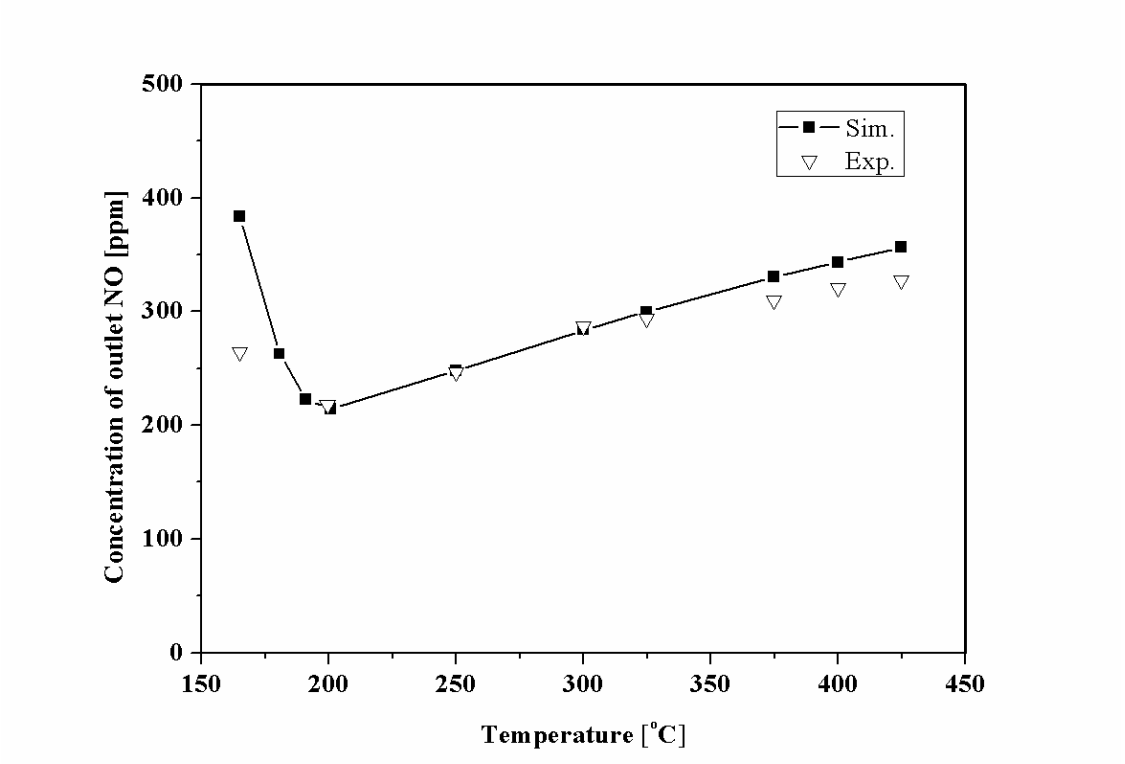

Figure 4-9 Average outlet NO concentration versus temperature, 60 s/5 s system. Conditions: Lean: H_2=2%, O_2=14.5%, NO=500 ppm, fill N_2; Rich: H_2=2%, NO=500 ppm, fill N_2.

NO is mainly converted to N_2, while only very little N_2O is produced (data not shown). Thus, the system has a high N_2 selectivity of more than 98%, which is quite advantageous compared with other catalytic systems, *e.g.* on Pt or on Pd [31, 56]. This supports the suggestion that such an after-treatment system is well suited for automotive applications. Drawbacks are the high price of rhodium as well as the short periods, which may deteriorate the fuel economy and are demanding to the electronic motor management.

From the comparison in Figure 4-9 it can be seen that the trend as well as the absolute values of the experimentally determined NO concentrations are reproduced well by DETCHEM^{TRANSIENT}. Merely in the high temperature region (above 300 °C) the simulations overestimate the experimentally determined emission.

The simulation results for the concentration of NO and N_2 at 300°C are plotted as a function of time in Figure 4-10. It should be mentioned that the simulation results show that N_2 is formed during both the lean and the rich periods for the investigated reactive system.

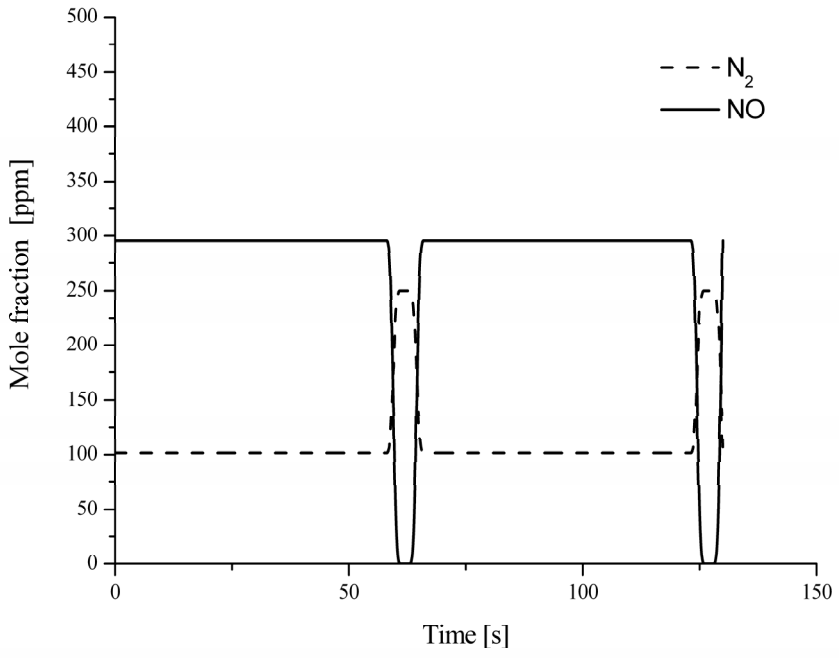

Figure 4-10 Time resolved NO and N_2 concentrations in the outlet gas at 300 ºC (simulation results). Conditions: Lean: H_2=2%, O_2=14.5%, NO=500 ppm, fill N_2; Rich: H_2=2%, NO=500 ppm, fill N_2.

Predicted Rhodium Surface Coverage

The predicted surface overlayer at 300 °C on rhodium is plotted as a function of time in Figure 4-11. It can be concluded that during the lean phase, the surface is mainly covered with oxygen species (θ_O = 0.70), while 29% of the surface remains uncovered. A comparison of the calculated surface overlayer with the calculated nitrogen formation shows that nitrogen forms simultaneous to the removal of oxygen from the surface (increase in vacant surface sites (Rh(s)), Figure 4-11). The nitrogen formation peaks during the rich period, simultaneously with the increase of the atomic nitrogen on the surface (N(s)) and the decrease of the oxygen coverage. The catalyst is moreover activated for further NO decomposition, because subsequent to the reduction of the surface more NO can adsorb. This activation is triggering the nitrogen formation during the oxygen-rich (lean) phase (Figure 4-10).

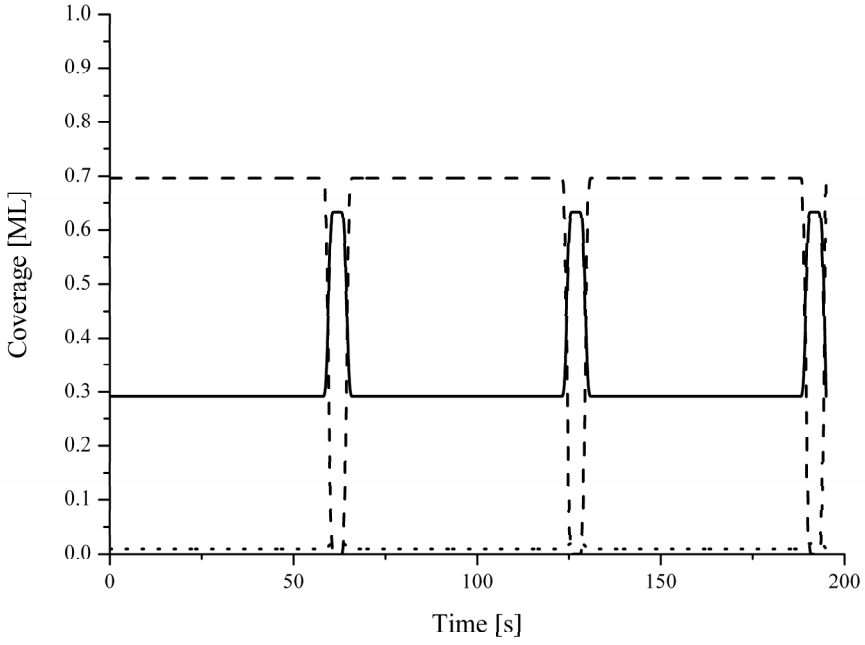

Figure 4-11 Predicted species surface coverage over time at 300 ºC for 60 s/5 s. (Simulation results). Solid line Rh(s) (vacant Rh surface), dashed line O(s) and dotted line N(s), ML means monolayer for the species coverage. Conditions: Lean: H_2=2%, O_2=14.5%, NO=500 ppm, fill N_2; Rich: H_2=2%, NO=500 ppm, fill N_2.

Effect of different lean/rich periods

To study the effect of different lean/rich periods, an analogous system with a lean period of 60 s and a rich period of 2 s is studied experimentally and theoretically. The results are

shown in Figure 4-12. The 60 s/2 s operation gives a lower NO conversion (about 26%) than the 60 s/5 s operation (with a conversion of 40%) within the temperature range investigated. The fuel consumption, however, would be much lower for this system, because the reductant-rich period is less than half as long, which requires less fuel. In the low temperature region around 200 °C, the activity of the catalytic system is slightly overestimated by the simulation, while at higher temperature (above 300 °C) the model underestimated the conversion of NO by less than 8%. Nevertheless, the simulations fit experimental observations well. Yet, considering that the 60 s/5 s system needs much more reductant to reduce/decompose the NO, it is less realistic to be adopted in a real vehicle compared to the 60 s/2 s system. Nevertheless, the study shows that the lean/rich ratio affects the NO conversion considerably and may be important for the catalyst practical use. Simulations could be coupled to algorithms for optimization to keep the NO_x conversion as high as possible and the fuel consumption (i.e. the length of the rich period) as low as possible.

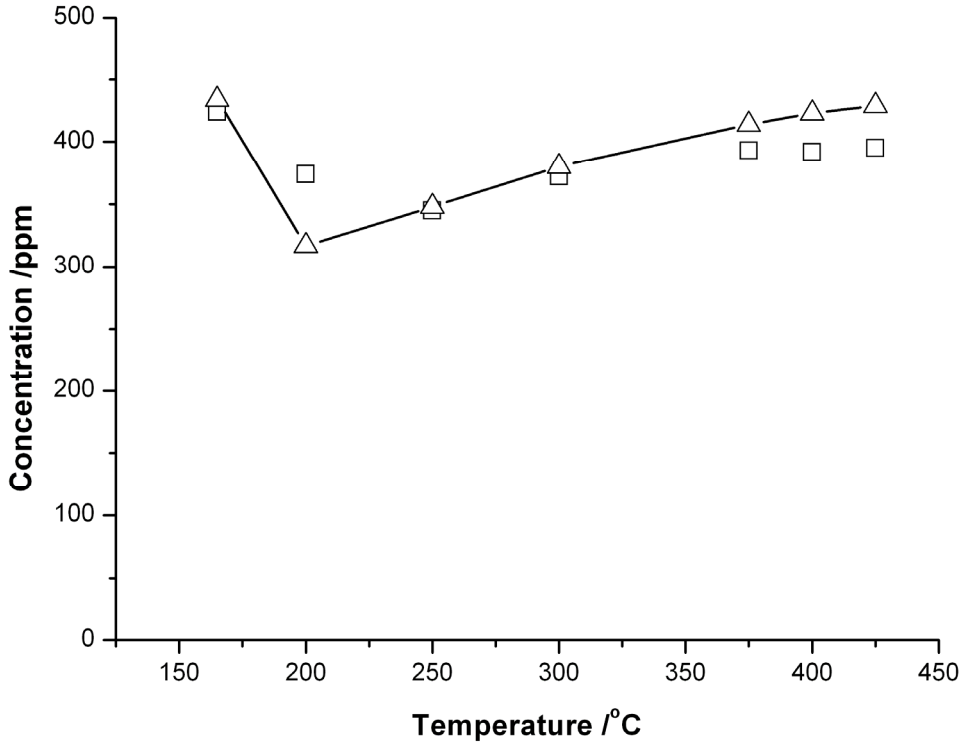

Figure 4-12 Temperature dependence of NO concentration, 60 s/2 s system. (Δ) Simulation results and (□) Experimental results. Conditions: Lean: H_2=2%, O_2=14.5%, NO=500 ppm, fill N_2; Rich: H_2=2%, NO=500 ppm, fill N_2.

4.3.5 NO-O_2 reactions over rhodium under steady-state conditions

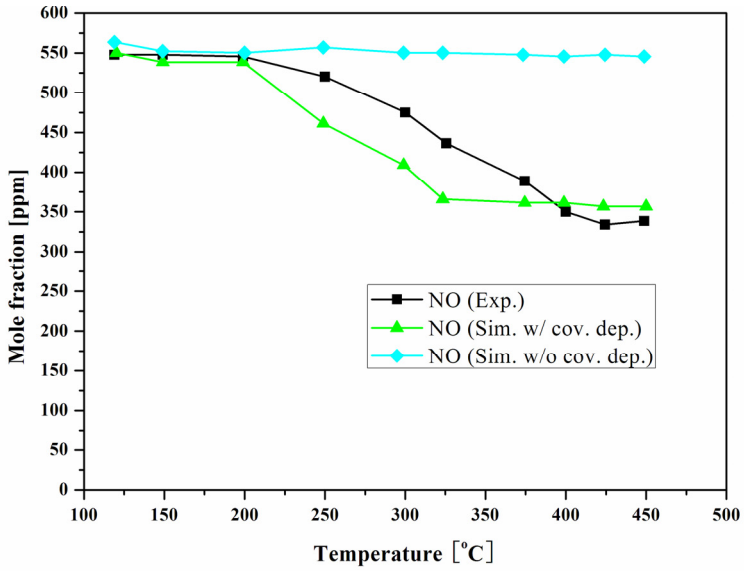

(a)

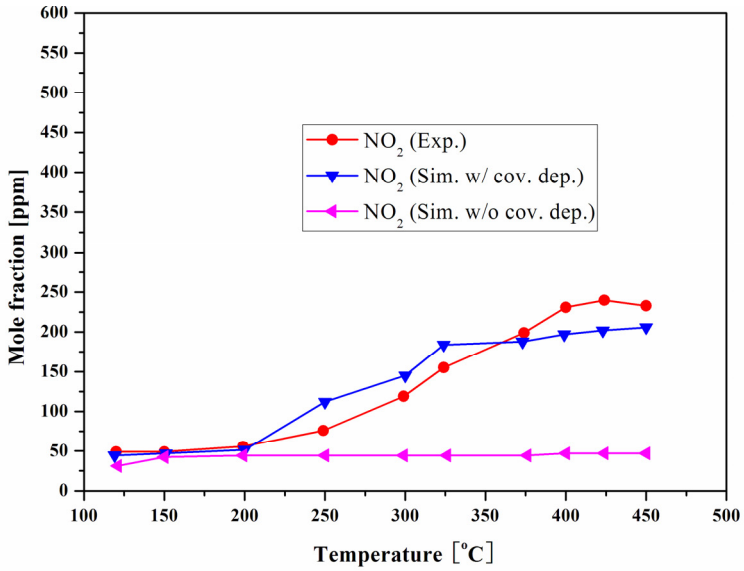

(b)

Figure 4-13 Mole fractions as a function of the temperature: (a) NO, and (b) NO_2. Comparison of experimental results to simulations based on a surface chemistry model with and without coverage-dependent kinetic parameters. Conditions: NO=550 ppm, NO_2=50 ppm, O_2=14%, fill N_2.

As stated in the earlier part, the coverage-dependent kinetics plays an important role in simulating the catalyst's behavior. NO oxidation into NO_2 over rhodium catalyst is investigated, as an example of the influence of coverage dependent kinetics. The conversion of a flow of 600 ppm NO_x (550 ppm NO and 50 ppm NO_2) and 14% O_2 in nitrogen were studied experimentally through the rhodium based catalyst under the condition stated before (see Chapter 4.3.1 Experimental). The simulation studies were performed with DETCHEM^{TRANSIENT} by taking the oxygen coverage dependent dissociation energy for molecular oxygen into account (see [5]).

The NO conversion and NO_2 formation were simulated as a function of temperature and were compared to experimental results. As can be seen from Figure 4-13, in the case in which activation of the NO oxidation with increasing oxygen coverage is not taken into account, simulations predict almost no conversion of NO to NO_2 absolutely, contrary to experimental observation. In case the activation is taken into account, the trend of the experimentally determined NO_2 formation and NO conversion is reproduced. These findings emphasize that coverage-dependent activation energies have to be taken into account in microkinetic modeling, in order to simulate conversions in catalytic converters accurately.

4.4 CO oxidation under transient lean-rich conditions: revisited

4.4.1 Effects of coverage-dependent activation energy

As stated earlier, the coverage-dependent kinetics plays an important role in simulating the catalyst's behavior. Here, the new results of simulations are compared to experimental observations and discussed considering such effects.

Experimental results [79] as well as DFT calculation [5] point towards a leveling-off of the oxygen at approximately 0.5 ML at room temperature. However, kinetic simulation of a stream of 2.5% oxygen in argon at 300 K shows that the rhodium surface is immediately covered by atomic oxygen due to a very fast dissociative adsorption of oxygen (circle-marked lines in Figure 4-14). However, Schwegmann *et al*. [80] were not able to prepare Rh(111) completely saturated with atomic oxygen even at elevated temperature (600 K) and with a strongly oxidizing agent (NO_2). Taking the oxygen coverage dependent dissociation energy for molecular oxygen into account (see [5]), shows that kinetic simulations support this

leveling-off (square marked lines in Figure 4-14, while the red line in the graph represents the experimental value).

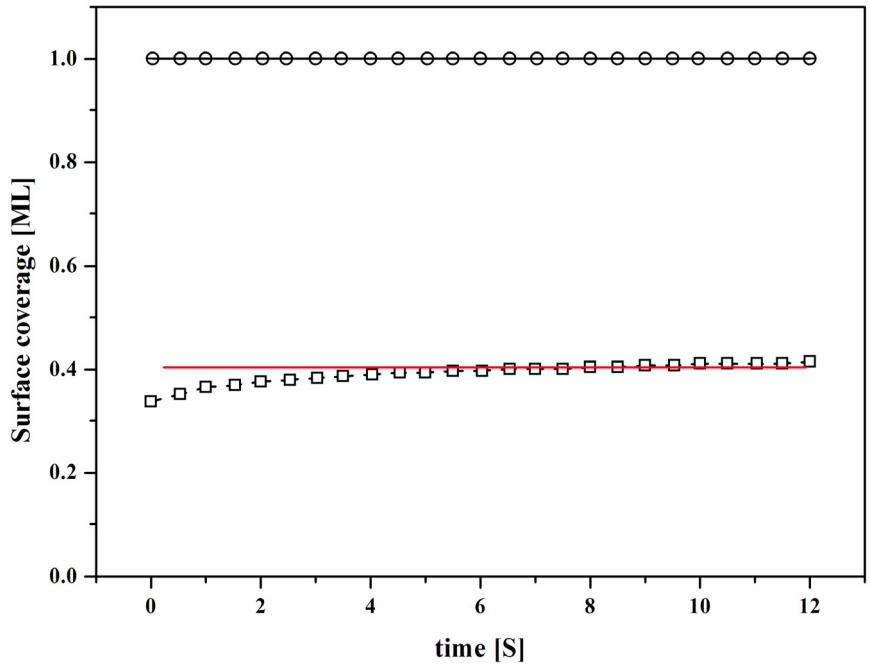

Figure 4-14 Comparison of the simulated surface coverages with and without accounting for surface coverage dependent kinetics [27]. Circle marked lines, O(s) with coverage independent kinetics; square marked lines, O(s) with oxygen coverage dependent kinetics.

This indicates that for predicting the surface occupation, coverage dependencies have to be taken into account. Furthermore, this could severely influence the overall behavior of transient processes since here one has to deal with fast changing surface compositions.

4.4.2 Implementation of the coverage-dependent activation energy

Based on the above results for the coverage-dependent activation energy for the oxygen adsorption, further simulation is conducted on the CO oxidation over rhodium under 60 s /5 s lean/rich periodic conditions as before. The mechanism is listed in the appendix, Table A-2.

Here, the inlet mole fraction of O_2 is taken as realistically measured in the experiments, see Figure 4-15. It is interesting to note that the O_2 concentration during the 5 s-rich periods in each cycle is non-zero, due to the response time of the switching valve.

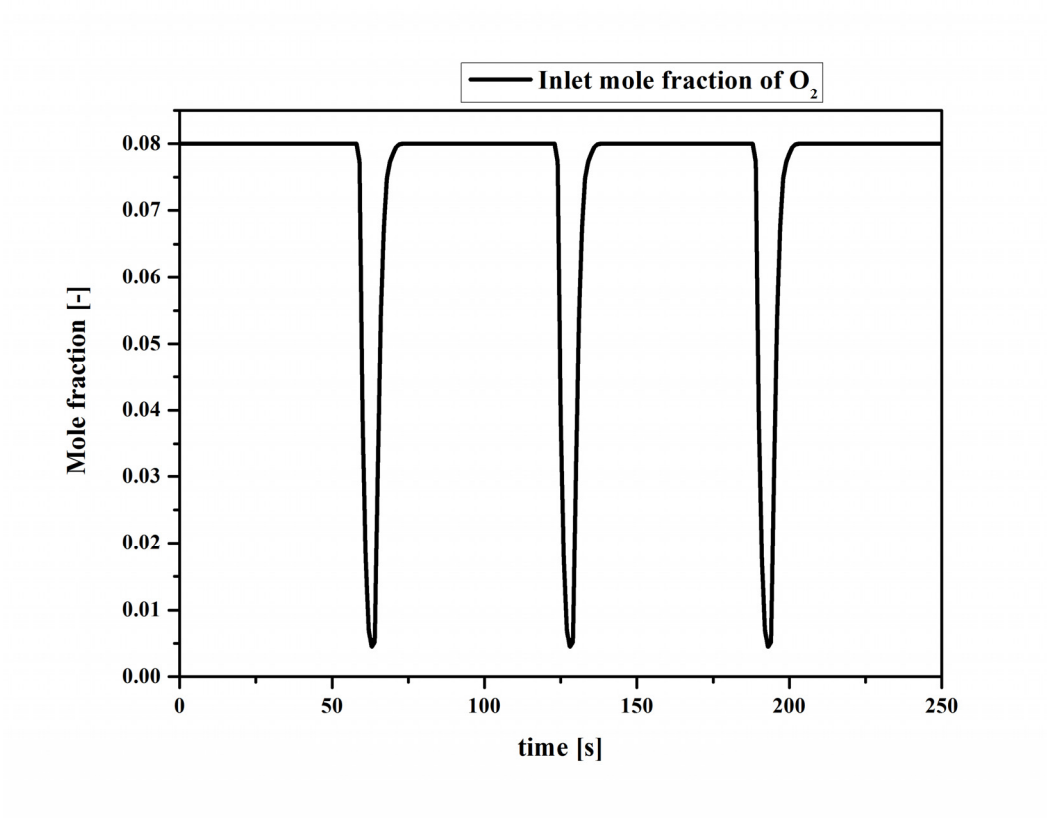

Figure 4-15 Realistic input inlet mole fraction of O_2, as measured in the experiments. Conditions: Lean/rich: 60 s/5 s, Lean: CO=0.5%, O_2=8%, fill N_2; Rich: CO=0.5%, fill N_2.

The transient CO conversion to CO_2 with the temperature is also investigated. At 250 ºC, during the transient from lean to rich periods, since there is less oxygen, the CO conversion begins to decrease, as shown in Figure 4-16, accompanied by the declined CO_2 formation. Then as the oxygen concentration begins to increase, the trend reverses.

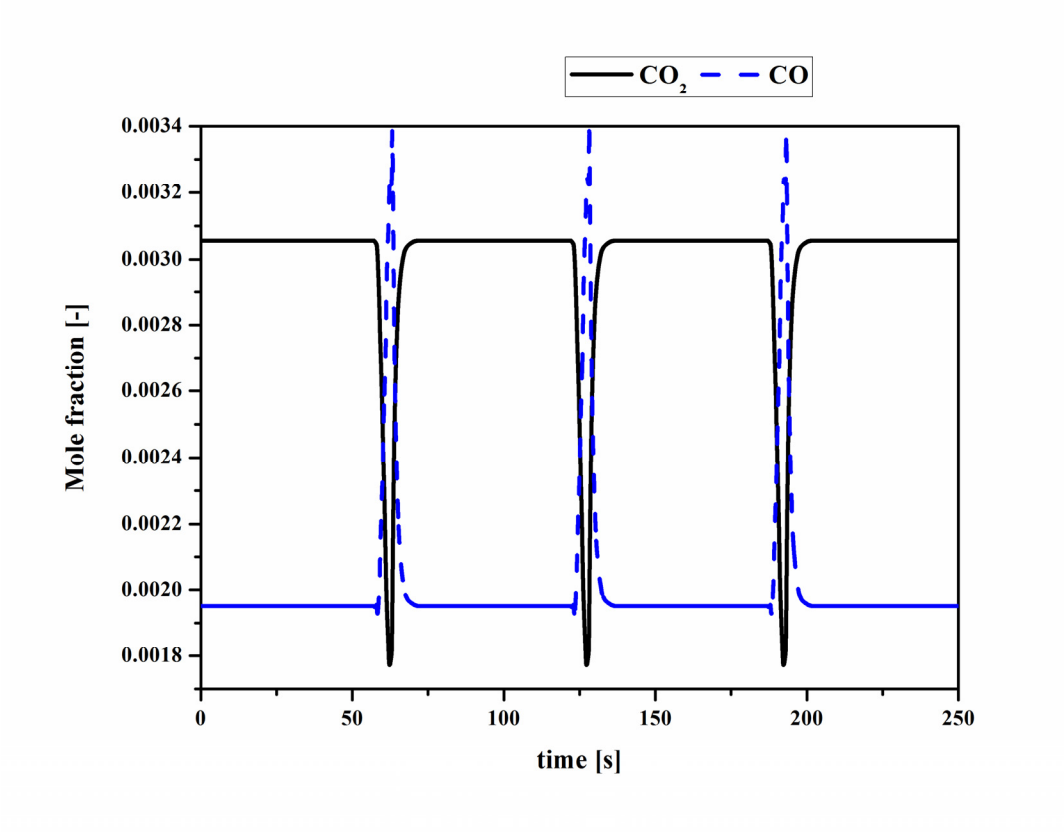

Figure 4-16 Predicted time resolved CO and CO_2 mole fractions in the outlet gas at 200 ºC. Conditions: Lean/rich: 60 s/5 s, Lean: CO=0.5%, O_2=8%, fill N_2; Rich: CO=0.5%, fill N_2.

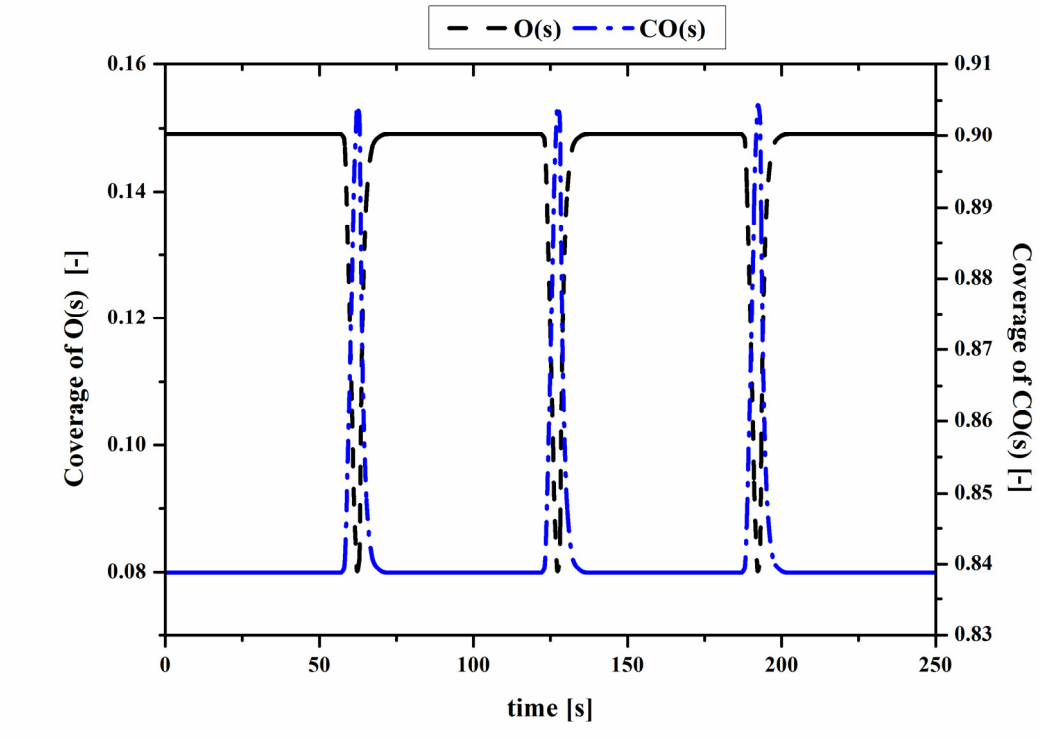

Figure 4-17 Predicted species surface coverage over time at 200 ºC for 60 s/5 s. Conditions: Lean/rich: 60 s/5 s, Lean: CO=0.5%, O_2=8%, fill N_2; Rich: CO=0.5%, fill N_2.

The time dependent coverages of the adsorbed species are shown in Figure 4-17. It is worth to note that with the improved mechanism, the maximum O coverage is below 0.5 ML for all the investigated temperatures. The rhodium surface is predominately covered by the adsorbed CO during the lean period at 200 ºC. However, during each lean-rich transient, the O coverage and the CO coverage change in an opposite way, which indicates the competitive adsorption of the two adsorbed species.

The overall CO conversions over the investigated temperatures are predicted with the new mechanism, as shown in Figure 4-18. It can be seen that the new mechanism predicted results much better than that shown in Figure 4-7: the CO conversion at higher temperatures above 250 ºC is reaching 100%. This agrees quantitatively with the experimental results, which shows the advantages of the improved mechanism for the transient simulation.

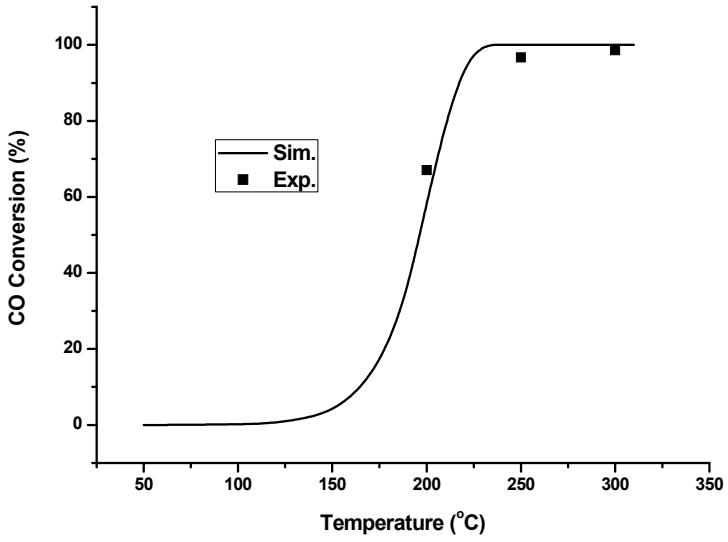

Figure 4-18 CO conversion versus temperature. Comparison of simulation with coverage-dependent and experimental results. Conditions: Lean/rich: 60 s/5 s, Lean: CO=0.5%, O_2=8%, fill N_2; Rich: CO=0.5%, fill N_2.

4.5 Analysis and discussion on the NO decomposition mechanism

A comparison of experimental and theoretical results presented in this chapter, supports the views that NO decomposition mechanism may follow the steps as below (based on the mechanism proposed by Nakatsuji *et al*.) [3, 26]:

(1) NO decomposition and subsequent N_2 (or N_2O) desorption;

(2) The left surface O generated from the above step accumulates on the metal surface and blocks the Rh surface by oxidation;

(3) Surface oxygen removal by reductant and/or maybe by surface O associative desorption as O_2, which needs further clarification leaves a reduced, clean Rh surface.

The rapid switching from lean to rich enables the removal of the surface O species so that the poisoning and deactivation by the surface O is avoided. The proposed mechanism of this Nakatsuji-type transient lean/rich NO decomposition/reduction system is completely different from that of NO_x Storage and Reduction (NSR) system. Therefore, it is anticipated that the former has good lasting conversion [2-5]. Especially in presence of SO_x, this advantage is presumably more pronounced.

4.6 Conclusions

This chapter presents the simulation of the transient processes during the catalytic decomposition of NO_x with CO/H_2 as reductants. The detailed microkinetic model developed in Chapter 3 is utilized to simulate several reaction systems with the transient module of DETCHEM - DETCHEM^{TRANSIENT}.

From the comparison of the theoretical and experimental results, the conclusion could be drawn that this code, in combination with an accurate detailed surface reaction mechanism, can well describe the transient behavior of the NO_x reduction/decomposition catalyst. It could support results published by Nakatsuji and co-workers, which show that by alternating the inlet gas composition periodically between lean and rich, NO_x can be efficiently decomposed/reduced with high selectivity towards N_2.

Furthermore, the results show that NO_x reduction by CO (CO-SCR/DeNO$_x$) under alternating lean/rich condition is not much feasible because of the low NO conversion for this studied system. However, a comparison of the results of the catalyst's activity with H_2 or CO as reductant, shows that hydrogen has generally a higher reduction capability, especially at low temperature. Hydrogen reforming could therefore be beneficial by enhancing the catalyst's performance during the start up period.

In addition, the simulation results for propene oxidation under steady state are included, which are validated against the experimental results from the literature. The incapability of the simple mechanism to predict the strong inhibition effects from the presence of NO may call for a more detailed mechanism for description of the NO reduction by propene in lean conditions.

Chapter 5: Conclusions and outlook

In this final chapter, the conclusions together with final remarks for the research are given. The outlook is depicted on the topic of the catalytic reduction of NO_x from the automotive exhaust gas.

In this thesis, a detailed microkinetic model is presented to study the transient behavior of the catalytic NO_x decomposition/reduction on a rhodium-based catalyst operated under periodic lean/rich conditions, as proposed by Nakatsuji [3]. This mechanism is utilized to simulate several reaction systems with the transient module of DETCHEM - DETCHEM^{TRANSIENT}. The reductants of CO and H_2 are used for the transient study.

The theoretical model is validated against the experimental results conducted by hte-company. The results could support those of Nakatsuji and co-workers, which show that by alternating the inlet gas composition periodically between lean and rich, NO_x can be efficiently decomposed/reduced with high selectivity towards N_2. Hydrogen production from on-board fuel reforming [81] could therefore be beneficial by enhancing the catalyst's low-

temperature activity during the cold-start period, especially under lean/rich periodic conditions.

As shown in this work, numerical simulation coupling with a detailed surface reaction mechanism offers a powerful alternative method for catalyst development and becomes more and more important. However, such detailed mechanism is still much lacking and not fully understood, in particular for the transient conditions. It is deemed that a better understanding should suggest ways to optimize the studied process. Therefore, apparently a detailed reaction mechanism together with an appropriate model is required for systematically designing and optimizing the catalyst and reactor. This work showed that the coupling of detailed reaction mechanisms with appropriate reactor models does help to understand the reactor behavior under transient conditions. Therefore, it potentially helps to understand the catalytic reactor over a wider range of realistic conditions.

The chemical modeler can contribute to bridging not only the pressure and material gaps, but also the possible existing gaps between the steady-state and the instationary kinetics, by combining the experimental investigations from the surface science community. Being of much significance, detailed experimental studies under both the stationary and the non-steady state conditions would be helpful for a deep and complete understanding to the lean catalytic $DeNO_x$ system. This contributes considerably to the discovery of more accurate heterogeneous reaction mechanism, and thus to improving the performance of the catalytic reactors.

Furthermore, the present study supports the following mechanism: The function of the very short reductant-rich pulses may be mainly the removal of the surface O species. The periodic removal of surface oxygen atoms by reductants prevents the catalyst from poisoning and consequent deactivation, assuring the durability of the catalyst. Furthermore, it is interesting to note that this switching also changes the coverages of different species on the rhodium surface with time. This is very important for minimizing the self-poisoning as stated before and regenerating the catalyst, in particular at low temperature. This is shown in the simulation results of the time dependent coverages. This illustrates one of the advantages of the transient running conditions on the catalytic system.

The discrepancy for modeling study with different lean/rich time spans indicates that the transient behavior is very complex. To better understand the kinetics for the system, a more detailed mechanism is needed. It is suggested that it should include the ammonia formation

and decomposition mechanism, as well as the intermediate reactions for the NO reduction by H_2 under the transient conditions. Furthermore, under the lean/rich cycles, oxidation state of the catalyst, i.e. metallic or metal oxide should be considered for further mechanism study. It should be mentioned that in the H_2-NO-O_2 system for example, in addition to the H_2 oxidation and NO reduction reactions considered, NH_x formation and decomposition will be involved by stepwise hydrogenation and dehydrogenation. Furthermore, the interaction among NO and NH_x should also be considered. In this work all these intermediate reactions are omitted due to the complexity and shortage of experimental data for validation, and are under investigation in an ongoing work [82].

As noted already, since the simple mechanism of propene oxidation can not predict the strong inhibition effects from the presence of NO, there is a need for a further detailed mechanism to describe the NO reduction by propene in an excess of oxygen. This will be realistic since propene is considered to be one of representative hydrocarbon species in the automotive exhaust gas. The removal of oxygen from the catalyst surface by hydrocarbons, e.g. propene, was meanwhile studied and will be included in further microkinetic investigations of a more realistic exhaust gas. Density-functional theory (DFT) calculations can contribute to the computing of the reaction energies involved in such a complex system.

Various researches show that the precious metal is indispensable for the exhaust gas purification, especially the rhodium as a good NO_x decomposition/reduction catalyst. Furthermore, facing the strong pressures from noble metal supply, it is imperative that Rh, Pt and Pd be utilized as effectively as possible for the catalytic control of automotive emissions [83]. One measure to this end is to gain a deeper and thorough understanding of the detailed reaction mechanisms concerning the precious metal catalyst utilized and thus to minimize the usage of such catalysts. Since the usage of the Pt, Pd and Rh is more and more, there is great need for the alternative metals as catalysts. Other precious metals, such as Ir, Au, Ag, or Ru are evaluated alone and in combination with Pt/Rh. In recent years Ir has been investigated with efforts by Toyota.

Bibliography

[1] W.S. Epling, L.E. Campbell, A. Yezerets, N.W. Currier, J.E. Parks II. *Overview of the Fundamental Reactions and Degradation Mechanisms of NO_x Storage/Reduction Catalysts*. Catalysis Reviews 46 (2), 163-245, 2004.

[2] S. Pischinger, M. Lamping, A. Sehr. *The Influence of pollutant emission reduction*. AutoTechnology, 6 (4), 48-51, August 2006.

[3] T. Nakatsuji, R. Yasukawa, K. Tabata, K. Ueda, M. Niwa. *A highly durable catalytic NOx reduction in the presence of SO_x using periodic two steps, an operation in oxidizing conditions and a relatively short operation in reducing conditions*. Applied Catalysis B: Environmental 21 (2), 121-131, 1999.

[4] Z.-P. Liu, S.J. Jenkins, D.A. King. *Car Exhaust Catalysis from First Principles: Selective NO Reduction under Excess O_2 Conditions on Ir*. Journal of the American Chemical Society 126 (34), 10746-10756, 2004.

[5] O.R. Inderwildi, D. Lebiedz, O. Deutschmann, J. Warnatz. *Coverage dependence of oxygen decomposition and surface diffusion on rhodium (111): a DFT study.* J Chem Phys 122 (3), 34710, 2005.

[6] O. Deutschmann, S. Tischer, S. Kleditzsch, C. Correa, D. Chatterjee, J. Warnatz. DETCHEM. http://www.detchem.com, Accessed in June 2004.

[7] E. Shustorovich. *The bond-order conservation approach to chemisorption and heterogeneous catalysis: applications and implications*. Advances in Catalysis, 37, 101-163, 1990.

[8] E. Shustorovich, H. Sellers. *The UBI-QEP method: A practical theoretical approach to understanding chemistry on transition metal surfaces*. Surface Science Reports 31 (1-3), 1-119, 1998.

[9] C.K. Narula, J.E. Allison, D.R. Bauer, H.S. Gandhi. *Materials Chemistry Issues Related to Advanced Materials Applications in the Automotive Industry*. Chemistry of Materials 8 (5), 984-1003, 1996.

[10] F. Kapteijn, J. Rodriguez-Mirasol, J.A. Moulijn. *Heterogeneous catalytic decomposition of nitrous oxide*. Applied Catalysis B: Environmental 9 (1-4), 25-64, 1996.

[11] J. Heywood, *Internal Combustion Engine Fundamentals*, McGraw Hill, Inc., New York, 1988.

[12] L.S. Glebov, A.G. Zakirova, V.F. Tret'yakov, T.N.Burdeinaya, G.S.Akopova. *State of the art of catalytic conversion of NO_x into N_2*. Petroleum Chemistry 42, 143-172, 2002.

[13] C.T. Bowman. *Control of combustion-generated nitrogen oxide emissions: Technology driven by regulation*. Proceedings of the Combustion Institute, 24, 859, 1993.

[14] M.V. Twigg. *Critical Topics in Exhaust Gas Aftertreatment*. Platinum Metals Review 45 (1), 176-178, 2001.

[15] M.P. Walsh. *Motor Vehicle Pollution Control*. Platinum Metals Review 44 (1), 22-30, 2000.

[16] C.D. Rakopoulos, E.G. Giakoumis, *Diesel Engine Transient Operation: Principles of Operation and Simulation Analysis*, Springer, 2009.

[17] P. Eastwood, *Critical Topics in Exhaust Gas Aftertreatment*, Research Studies Press Ltd., Baldock, Hertfordshire, England, 2000.
[18] R. Heck, R. Farrauto. *Automotive catalysts*. Automotive Engineering 104 (2), 93-96, 1996.
[19] B.I. Bertelsen. *The U.S. Motor Vehicle Emission Control Program*. Platinum Metals Review 45 (2), 50-59, 2001.
[20] D.A. King. *Environment - Climate change science: Adapt, mitigate, or ignore?* Science 303 (5655), 176-177, 2004.
[21] R.J. Farrauto, R.M. Heck. *Environmental catalysis into the 21st century*. Catalysis Today 55 (1-2), 179-187, 2000.
[22] R.M. Heck, R.J. Farrauto. *Automobile exhaust catalysts*. Applied Catalysis A: General 221 (1-2), 443-457, 2001.
[23] S.i. Matsumoto. *Catalytic Reduction of Nitrogen Oxides in Automotive Exhaust Containing Excess Oxygen by NOx Storage-Reduction Catalyst* CATTECH 4 (2), 102-109, 2000.
[24] R.M. Heck, R.J. Farrauto, S.T. Gulati, *Catalytic Air Pollution Control*, 2nd Edition, Wiley-Interscience, 2002.
[25] E. Fridell, M. Skoglundh. *Model studies of sulphur deactivation of NOx storage catalysts*. Society of Automotive Engineers, [Special Publication] SP-1835 (Diesel Emissions), 109-113, 2004.
[26] T. Nakatsuji, J. Ruotoistenmaki, V. Komppa, Y. Tanaka, T. Uekusa. *A catalytic NO reduction in periodic lean and rich excursions over Rh supported on oxygen storage capacity materials*. Applied Catalysis B: Environmental 38 (2), 101-116, 2002.
[27] O.R. Inderwildi. *Multiscale modeling for automotive exhaust-gas aftertreatment - from the quantum chemistry to the engineering level*. PhD thesis, University of Heidelberg, Heidelberg, 2005.
[28] A.P. Kieboom, J.A. Moulijn, P.W.N.M.v. Leeuwen, R.A.v. Santen. *History of Catalysis*. In: J. A. Moulijn, P. W. N. M. v. Leeuwen, R. A. v. Santen, and B. A. Averill (Eds.), Catalysis: An Integrated Approach, Elsevier, Amsterdam, p. 3-28, 1999.
[29] P.-A. Carlsson, P. Thormählen, M. Skoglundh, H. Persson, E. Fridell, E. Jobson, B. Andersson. *Periodic Control for Improved Low-Temperature Catalytic Activity*. Topics in Catalysis 16-17 (1), 343-347, 2001.
[30] J. Wei. *Catalysis for motor vehicle emissions*. In: D. D. Eley, H. Pines, and B. W. Paul (Eds.), Advances in Catalysis, Academic Press, p. 57-129, 1975.
[31] R. Burch, M.D. Coleman. *An investigation of the $NO/H_2/O_2$ reaction on noble-metal catalysts at low temperatures under lean-burn conditions*. Applied Catalysis B: Environmental 23 (2-3), 115-121, 1999.
[32] M. Skoglundh, P. Thormahlen, E. Fridell, F. Hajbolouri, E. Jobson. *Improved light-off performance by using transient gas compositions in the catalytic treatment of car exhausts*. Chemical Engineering Science 54 (20), 4559-4566, 1999.
[33] J.F. Haw, *In-Situ Spectroscopy in Heterogeneous Catalysis*, Wiley-VCH, 2002.
[34] E.C. Su, W.G. Rothschild, H.C. Yao. *CO oxidation over Pt/gama-Al_2O_3 under high pressure*. Journal of Catalysis 118 (1), 111-124, 1989.
[35] R.D. H. Randall, A. Renken,. *Model discrimination by unsteady-state operation: Application to the reduction of NO with CO on iron oxide*. The Canadian Journal of Chemical Engineering 74 (5), 586-593, 1996.
[36] D. Na-Ranong, R. Yuangsawad, P. Kitchaiya, T. Aida. *Application of periodic operation to kinetic study of NO-CO reaction over Rh/Al_2O_3*. Chemical Engineering Journal 146 (2), 275-286, 2009.

[37] C.O. Bennett. *Experiments and Processes in the Transient Regime for Heterogeneous Catalysis*. In: W. O. Haag, B. C. Gates, and K. Helmut (Eds.), Advances in Catalysis, Academic Press, Volume 44, p. 329-416, 1999.
[38] O. Deutschmann, J. Warnatz. *Diagnostics for Catalytic Combustion*. In: K. Kohse-Hoeinghaus and J. B. Jeffries (Eds.), Applied Combustion Diagnostics, Taylor and Francis Publ., p. 518-533, 2002.
[39] D.K. Zerkle, M.D. Allendorf, M. Wolf, O. Deutschmann. *Understanding Homogeneous and Heterogeneous Contributions to the Platinum-Catalyzed Partial Oxidation of Ethane in a Short-Contact-Time Reactor*. Journal of Catalysis 196 (1), 18-39, 2000.
[40] O. Deutschmann, S. Tischer, S. Kleditzsch, C. Correa, D. Chatterjee, J. Warnatz. DETCHEM. http://www.detchem.com, Accessed in 2005.
[41] K.N. Pattas, A.M. Stamatelos, P.K. Pistikopoulos, G.C. Koltsakis, P.A. Konstandinidis, E. Volpi, E. Leveroni. *Transient Modeling of 3-Way Catalytic Converters*. SAE Paper 940934 1994.
[42] S. Tischer, O. Deutschmann. *Recent advances in numerical modeling of catalytic monolith reactors*. Catalysis Today 105 (3-4), 407-413, 2005.
[43] J. Windmann, J. Braun, P. Zacke, D. Chatterjee, O. Deutschmann, J. Warnatz. *Impact of the Inlet Flow Distribution on the Light-Off Behavior of a 3-Way Catalytic Converter*. SAE Technical Paper Series No. 2003-01-0937, 2003.
[44] S. Tischer, C. Correa, O. Deutschmann. *Transient three-dimensional simulations of a catalytic combustion monolith using detailed models for heterogeneous and homogeneous reactions and transport phenomena.* Catalysis Today 69 (1-4), 57-62, 2001.
[45] *Fluent Version 5.0*, FLUENT Inc., Lebanon, New Hampshire, 1998.
[46] L.L. Raja, R.J. Kee, O. Deutschmann, J. Warnatz, L.D. Schmidt. *A critical evaluation of Navier-Stokes, boundary-layer, and plug-flow models of the flow and chemistry in a catalytic-combustion monolith*. Catalysis Today 59 (1-2), 47-60, 2000.
[47] L.J. Broadbelt, D.J. Klinke, *Kinetics of Catalyzed Reactions–Heterogeneous, Section: Introduction*. Encyclopedia of Catalysis, 2002.
[48] R. Kissel-Osterrieder, F. Behrendt, J. Warnatz, U. Metka, H.-R. Volpp, J. Wolfrum, *Experimental and Theoretical Investigation of CO-Oxidation on Platinum: Bridging the Pressure and the Materials Gap*. Proceedings of the Combustion Institute 28, 1331-1339, 2000.
[49] H.-R. Volpp, J. Wolfrum. *Sum-Frequency Generation (SFG) Vibrational Spectroscopy as a Means for the Investigation of Catalytic Combustion*. In: K. Kohse-Hoeinghaus and J. B. Jeffries (Eds.), Applied Combustion Diagnostics, Taylor and Francis Publ., p. 336-358, 2002.
[50] T. Pery, M.G. Schweitzer, H.R. Volpp, J. Wolfrum, L. Ciossu, O. Deutschmann, J. Warnatz. *Sum-frequency generation in situ study of CO adsorption and catalytic CO oxidation on rhodium at elevated pressures*. Proceedings of the Combustion Institute 29 (1), 973-980, 2002.
[51] G. Ertl. *Dynamics of reactions at surfaces*. In: B. C. Gates and H. Knoezinger (Eds.), Advances in Catalysis, Academic Press, p. 1-69, 2000.
[52] J.A. Dumesic, D.F. Rud, L.M. Aparicio, J.E. Rekoske, A.A. Revino, *The Microkinetics of Heterogeneous Catalysis*, American Chemical Society, Washington, D.C., 1993.
[53] S. Derrouiche, D. Bianchi. *Experiments and kinetic model regarding the induction period observed during the oxidation by O_2 of adsorbed CO species on Pt/Al_2O_3 catalysts*. Journal of Catalysis 230 (2), 359-374, 2005.
[54] T. Nakatsuji, J. Ruotoistenmaki, M. Matsubara, T. Uekusa, Y. Tanaka. *A new transient NO_x direct catalytic decomposition on a Rh-based catalyst*. 2003.
[55] O. Deutschmann, R. Schwiedernoch, L.I. Maier, D. Chatterjee. *Natural Gas Conversion in Monolithic Catalysts: Interaction of Chemical Reactions and Transport Phenomena.* In: E.

Iglesia, J. J. Spivey, and T. H. Fleisch (Eds.), Natural Gas Conversion VI, Elsevier, p. 251-258, 2001.
[56] D. Chatterjee, O. Deutschmann, J. Warnatz. *Detailed surface reaction mechanism in a three-way catalyst*. Faraday Discussions 119, 371-384, 2001.
[57] L. Olsson. *Fundamental Studies of Catalytic NO_x Removal - Micro Kinetic Modeling, Monte Carlo Simulations and Flow Reactor Experiments*. PhD thesis, Chalmers University of Technology, Gothenbourg, 2002.
[58] H. Sellers, E. Shustorovich. *Intrinsic activation barriers and coadsorption effects for reactions on metal surfaces: unified formalism within the UBI-QEP approach*. Surface Science 504 (1-3), 167-182, 2002.
[59] R.J. Madix, J. Benziger. *Kinetic Processes on Metal Single-Crystal Surfaces*. Annual Review of Physical Chemistry 29 (1), 285-306, 1978.
[60] J.B. Benziger. *Thermodynamics of adsorption of diatomic molecules on transition metal surfaces*. Applications of Surface Science 6 (2), 105-121, 1980.
[61] S.B. Schwartz, G.B. Fisher, L.D. Schmidt. *Nitric oxide + carbon monoxide on rhodium(111): steady-state rates and adsorbate coverages*. J. Phys. Chem. 92 (2), 389-395, 1988.
[62] T. Nobukawa, M. Yoshida, S. Kameoka, S.-i. Ito, K. Tomishige, K. Kunimori. *Role of nascent oxygen transients in N_2O decomposition and selective catalytic reduction of N_2O*. Catalysis Today 93-95 791-796, 2004.
[63] A.V. Zeigarnik. *Adsorption and Reactions of N_2O on Transition Metal Surfaces*. Kinetics and Catalysis 44 (2), 233 - 246, 2003.
[64] R. Weber. Microkinetics of catalytic processes. 1st crosscut workshop on lean emissions reduction simulations. 2001.
[65] Y.-F.Y. Yao. *The oxidation of CO and hydrocarbons over noble metal catalysts*. Journal of Catalysis 87 (1), 152-162, 1984.
[66] Y.-F.Y. Yao. *Oxidation of Alkanes over Noble Metal Catalysts*. Industrial & Engineering Chemistry Product Research and Development 19 (3), 293-298, 1980.
[67] W.C. Hecker, A.T. Bell. *Reduction of NO by H_2 over silica-supported rhodium: Infrared and kinetic studies*. Journal of Catalysis 92 (2), 247-259, 1985.
[68] T. Nakatsuji, V. Komppa. *A catalytic NO_x reduction system using periodic two steps: an operation in oxidizing conditions and a relatively short operation in reducing conditions*. Applied Catalysis B: Environmental 30 (1-2), 209-223, 2001.
[69] T. Nakatsuji, J. Ruotoistenmaki, M. Matsubara, T. Uekusa, Y. Tanaka. *A new transient NOx direct catalytic decomposition on a Rh-based catalyst*. SAE Technical Paper Series No. 2003-01-3243, 2003.
[70] T. Engel, G. Ertl. *Elementary Steps in the Catalytic Oxidation of Carbon Monoxide on Platinum Metals*. In: D. D. Eley, H. Pines, and B. W. Paul (Eds.), Advances in Catalysis, Academic Press, p. 1-78, 1979.
[71] G.B. Fisher, S.H. Oh, J.E. Carpenter, C.L. Dimaggio, S.J. Schmieg, D.W. Goodman, T.W. Root, S.B. Schwartz, L.D. Schmidt. *Mechanisms of the Carbon Monoxide Oxidation and Nitric Oxide Reduction Reactions over Single Crystal and Supported Rhodium Catalysts: High Pressure Rates Explained Using Ultrahigh Vacuum Surface Science*. In: A. Crucq and A. Frennet (Eds.), Studies in Surface Science and Catalysis, Elsevier, p. 215-220, 1987.
[72] S.H. Oh, G.B. Fisher, J.E. Carpenter, D.W. Goodman. *Comparative kinetic studies of CO-O_2 and CO-NO reactions over single crystal and supported rhodium catalysts*. Journal of Catalysis 100 (2), 360-376, 1986.
[73] B.K. Cho. *Mechanistic Importance of Intermediate N_2O + CO Reaction in Overall NO + CO Reaction System: II. Further Analysis and Experimental Observations*. Journal of Catalysis 148 (2), 697-708, 1994.

[74] V.P. Zhdanov. *Does the N_2O-CO Subreaction Play an Important Role in the NO-CO Reaction on Rh?* Journal of Catalysis 162 (1), 147-148, 1996.
[75] B.K. Cho, B.H. Shank, J.E. Bailey. *Kinetics of NO reduction by CO over supported rhodium catalysts: Isotopic cycling experiments*. Journal of Catalysis 115 (2), 486-499, 1989.
[76] A.A. Nikolopoulos, E.S. Stergioula, E.A. Efthimiadis, I.A. Vasalos. Catalysis Today 54 (4), 439, 1999.
[77] E.A. Efthimiadis, S.C. Christoforou, A.A. Nikolopoulos, I.A. Vasalos. Applied Catalysis B: Environmental 22 (2), 91, 1999.
[78] S.H. Oh, J.E. Carpenter. *Role of NO in inhibiting CO oxidation over alumina-supported rhodium*. Journal of Catalysis 101 (1), 114-122, 1986.
[79] M.V. Ganduglia-Pirovano, M. Scheffler. *Structural and electronic properties of chemisorbed oxygen on Rh(111)*. Physical Review B 59 (23), 15533-15543, 1999.
[80] S. Schwegmann, H. Over, V. De Renzi, G. Ertl. *The atomic geometry of the O and CO + O phases on Rh(111).* Surface Science 375 (1), 91-106, 1997.
[81] S. Sitshebo, A. Tsolakis, U. Elghawi, K. Theinnoi, M.L. Wyszynski, R.F. Cracknell, R.H. Clark. *Hydrogen rich gas production in a diesel partial oxidation reactor with HC speciation*. SAE Technical Paper Series No.2009-01-0276, 2009.
[82] Q. Su, O. Deutschmann, J. Warnatz. Unpublished results. 2009.
[83] C.H.F. Peden, D.N. Belton, S.J. Schmieg. *Structure Sensitive Selectivity of the NO-CO Reaction over Rh(110) and Rh(111)*. Journal of Catalysis 155 (2), 204-218, 1995.

Appendences

Table A-1 Surface reaction mechanisms of CO oxidation, H_2 oxidation and NO reduction on Rh for transient simulation in Chapter 4 (on the basis of open literature data, new calculations with UBI-QEP and simulation fits to the transient experimental results).

No.	Reaction		A, S_0	β	E_a	ε_i, μ_i
(a) O_2-Rh system						
A. Adsorption						
(1)	$O_2 + 2Rh(s)$	$\rightarrow 2O(s)$	$S_0 = 1.00 \times 10^{-2}$	0.0	0.0	
B. Desorption						
(2)	$2O(s)$	$\rightarrow O_2 + 2Rh(s)$	3.00×10^{21}	0.0	293.3	
(b) CO-O_2-Rh system						
A. Adsorption						
(3)	$CO + Rh(s)$	$\rightarrow CO(s)$	$S_0 = 5.00 \times 10^{-1}$	0.0	0.0	
B. Desorption						
(4)	$CO(s)$	$\rightarrow CO + Rh(s)$	1.00×10^{14}	0.0	132.3	
$CO(s)						18.8
$N(s)						41.9
C. Surface reaction						
(5)	$CO(s) + O(s)$	$\rightarrow CO_2 + 2Rh(s)$	$3.70 \times 10^{+20}$	0.0	59.9	
(c) H_2-O_2-Rh system						
A. Adsorption						
(6)	$H_2 + 2Rh(s)$	$\rightarrow 2H(s)$	$S_0 = 1.50 \times 10^{-2}$	0.0	0.0	
(7)	$H_2O + Rh(s)$	$\rightarrow H_2O(s)$	$S_0 = 1.00 \times 10^{-1}$	0.0	0.0	
B. Surface reaction						
(8)	$H(s) + O(s)$	$\rightarrow OH(s) + Rh(s)$	5.00×10^{22}	0.0	83.7	
(9)	$OH(s) + Rh(s)$	$\rightarrow H(s) + O(s)$	3.00×10^{20}	0.0	37.7	
(10)	$OH(s) + H(s)$	$\rightarrow H_2O(s) + Rh(s)$	3.00×10^{20}	0.0	33.5	
(11)	$H_2O(s) + Rh(s)$	$\rightarrow OH(s) + H(s)$	5.00×10^{22}	0.0	106.4	
(12)	$2OH(s)$	$\rightarrow H_2O(s) + O(s)$	3.00×10^{21}	0.0	100.8	
(13)	$H_2O(s) + O(s)$	$\rightarrow 2OH(s)$	3.00×10^{21}	0.0	224.2	
C. Desorption						
(14)	$2H(s)$	$\rightarrow H_2 + 2Rh(s)$	3.00×10^{21}	0.0	77.8	
(15)	$H_2O(s)$	$\rightarrow H_2O + Rh(s)$	3.00×10^{13}	0.0	45.0	
(d) NO-N_2O-N_2-O_2-Rh system						
A. Adsorption						
(16)	$NO + Rh(s)$	$\rightarrow NO(s)$	$S_0 = 5.00 \times 10^{-1}$	0.0	0.0	
(17)	$N_2O + Rh(s)$	$\rightarrow N_2O(s)$	$S_0 = 5.00 \times 10^{-1}$	0.0	0.0	
B. Desorption						
(18)	$NO(s)$	$\rightarrow NO + Rh(s)$	5.00×10^{13}	0.0	108.9	
(19)	$N_2O(s)$	$\rightarrow N_2O + Rh(s)$	1.00×10^{13}	0.0	50.0	

(20) N(s) + N(s)	→ N_2 + 2Rh(s)	1.11×10^{19}	0.0	136.9	
	$N(s)				16.7
C. Surface reaction					
(21) NO(s) + Rh(s)	→ N(s) + O(s)	2.22×10^{20} (a)	0.0	79.5	
	$NO(s)				-20 (b)
	$N(s)				-20 (c)
(22) NO(s) + N(s)	→ N_2O(s) + Rh(s)	3.70×10^{21}	0.0	79.5	
(23) N_2O(s)	→ N_2 + O(s)	6.50×10^{13}	0.0	73.2	

Note:

1) According to the Equation shown below, the units of A are give in terms of mol, cm and s, β in [-], E_a and ε_i are in kJ/mol.
$k_k^{(s)} = A_k T^{\beta_k} \exp(-\frac{E_{a,k}}{RT}) \prod_{i=1}^{N_s} \Theta_i^{\mu_{ik}} \exp(\frac{\varepsilon_{ik}\Theta_i}{RT})$

2) Rh(s) denotes a free adsorption site on solid rhodium, species followed by (s) denote that they are adsorbed on a such a solid rhodium adsorption sites (Rh(s)), e.g., NO(s) denotes NO adsorbed on Rh(s). Within the mean field approach the surface is considered uniform and therefore only one possible adsorption site (Rh(s)) is given.

3) For the lean/rich ratio of 60 s/2 s, different data are used: for (a), 2.22 × 10+22, for (b), 0 and for (c), 0, details referring the text.

Table A-2 Surface reaction mechanisms of CO oxidation on Rh for transient simulation in Chapter 4 considering the coverage-dependent kinetics.

No.	**Reaction**		***A* (mol, cm, s), S_0 (-)**	**β (-)**	**E_a (kJ/mol)**	**ε_i (kJ/mol), μ_i (-)**	**Note**
A. Adsorption							
(1)	O_2 + 2Rh(s)	→ 2O(s)	$S_0 = 1.00 \times 10^{-2}$	0.0	0.0		
	$O(s)					-115.0	[27]
(2)	CO + Rh(s)	→ CO(s)	$S_0 = 5.00 \times 10^{-1}$	0.0	0.0		
B. Desorption							
(3)	2O(s)	→ O_2 + 2Rh(s)	3.00×10^{21}	0.0	293.3		
	$O(s)					115.0	[27]
(4)	CO(s)	→ CO + Rh(s)	1.60×10^{14}	0.0	132.3		
	$CO(s)					40	This work
C. Reaction							
(5)	CO(s) + O(s)	→CO_2 + 2Rh(s)	4.78×10^{18}	0.0	59.9		This work

Note:

According to the Equation shown below, the units of A are give in terms of mol, cm and s, β in [-], E_a and ε_i are in kJ/mol.
$k_k^{(s)} = A_k T^{\beta_k} \exp(-\frac{E_{a,k}}{RT}) \prod_{i=1}^{N_s} \Theta_i^{\mu_{ik}} \exp(\frac{\varepsilon_{ik}\Theta_i}{RT})$

Acknowledgements

When the thesis is finishing, I would like to express my greatest gratitude to the following people who have helped me quite a lot and made this work possible:

Prof. Dr. Dr. h.c. Jürgen Warnatz, my former supervisor, who left us too early, for providing me the employment and the interesting research topics, and for teaching me quite a lot during the past years, which will help me for the following years;

Prof. Dr. Uwe Riedel for fruitful discussions, critical reading and corrections, and constructive suggestions in my thesis and everyday administrative help;

Prof. Dr. Jürgen Wolfrum for his interest in my work, warm-hearted great help and support to me, agreeing to be my examiner, and timely discussions;

Prof. Dr. Olaf Deutschmann for his continuous support to my research in this fascinating field and critical suggestions to my work;

Prof. Dr. Dr. h.c. Hans Georg Bock for his great help and strong support in my study in IWR;

Dr. Oliver R. Inderwildi and PD. Dr. Dirk Lebiedz for cooperation and great help within the ConNeCat project;

Dr. Steffen Tischer, for timely solutions to my questions on DETCHEM; PD. Dr. Wolfgang Bessler for interesting discussions; Mrs. Ingrid Hellwig for her kindness and everyday help, Mrs. Barbara Werner, Mrs. Margret Rothfuss, Mrs. Sylvia Boganski for their kind help during my stay in IWR; Mr. Sven Sanwald, my office roommate and all the people in the group Reaflow (Reaktive Strömung) at IWR for friendship and help during my stay in Heidelberg;

Prof. Dr. Hans-Robert Volpp, Dr. W. Strehlau, Dr. O. Gerlach, Dipl.-Ing. J. Maier, Dr. F. Rohr for discussions and help within the ConNeCat project.

My friends in Chinese community in Heidelberg and my former friends in China for their friendship and help, and my students in Dalian for their help in my study and work;

My former professors in China, especially Prof. Jiahua Chen, Associate Prof. Guochao Zhu, Prof. Xiyan Gao, Prof. Maozhao Xie, Prof. Xigeng Song and Prof. Yongchen Song (DUT); Prof. Huamin Zhang and Prof. Can Li (DICP); Prof. Xuchang Xu, Prof. Jianxin Wang, and Prof. Qiang Yao (Tsinghua), Prof. Zhen Huang and Prof. Xinqi Qiao (SJTU) for their lasting encouragement and great help during my study and work in China and in Heidelberg;

Last but not least, my parents, my elder sisters and younger brother for their lasting love, care, support, understanding, and encouragement throughout my living and studying during the long years; and my wife, Zhongyan for her deep love, understanding and strong support, especially during the hard times. This thesis is dedicated to all my family!

The present work is partially supported by German Federal Ministry of Education and Research (BMBF) via ConNeCat lighthouse project “Automotive exhaust catalyst” and also by Heidelberg Graduate School (HGS) of Mathematical and Computational Methods. Both funding bodies are acknowledged for the financial support.

Erklärung

Hiermit versichere ich, dass ich diese Arbeit selbstständig verfasst habe und keine anderen als die angegebenen Quellen und Hilfsmittel verwendet habe.

Heidelberg, den

Qingyun Su